Journal of Medicinal Chemistry

Article

pubs.acs.org/jmc

Discovery of a Novel Class of Highly Potent, Selective, ATP-Competitive, and Orally Bioavailable Inhibitors of the Mammalian Target of Rapamycin (mTOR)

Craig S. Takeuchi, Byung Gyu Kim,*,† Charles M. Blazey, Sunghoon Ma, Henry W. B. Johnson, Neel K. Anand, Arlyn Arcalas, Tae Gon Baik, Chris A. Buhr, Jonah Cannoy, Sergey Epshteyn, Anagha Joshi, Katherine Lara, Matthew S. Lee, Longcheng Wang, James W. Leahy,*,‡ John M. Nuss, Naing Aay, Ron Aoyama, Paul Foster, Jae Lee, Isabelle Lehoux, Narsimha Munagala, Arthur Plonowski, Sharmila Rajan, John Woolfrey, Kyoko Yamaguchi, Peter Lamb, and Nicole Miller

Department of Drug Discovery, Exelixis, 169 Harbor Way, South San Francisco, California 94083, United States

ABSTRACT: A series of novel, highly potent, selective, and ATP-competitive mammalian target of rapamycin (mTOR) inhibitors based on a benzoxazepine scaffold have been identified. Lead optimization resulted in the discovery of inhibitors with low nanomolar activity and greater than 1000-fold selectivity over the closely related PI3K kinases. Compound **28** (XL388) inhibited cellular phosphorylation of mTOR complex 1 (p-p70S6K, pS6, and p-4E-BP1) and mTOR complex 2 (pAKT (S473)) substrates. Furthermore, this compound displayed good pharmacokinetics and oral exposure in multiple species with moderate bioavailability. Oral administration of compound **28** to athymic nude mice implanted with human tumor xenografts afforded significant and dose-dependent antitumor activity.

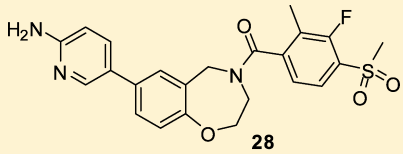

mTOR	IC50	9.9 nM
PI3Kα	IC50	>3,000 nM
PI3Kβ	IC50	>5,000 nM
PI3Kγ	IC50	>5,000 nM
PI3Kδ	IC50	>5,000 nM

INTRODUCTION

The mammalian target of rapamycin (mTOR) is a large protein kinase that integrates both extracellular and intracellular signals of cellular growth, proliferation, and survival. Both extracellular mitogenic growth factor signaling from cell surface receptors and intracellular signals that convey hypoxic stress, energy, and nutrient status converge at mTOR.[1−4] mTOR exists in two distinct multiprotein complexes: mTOR complex 1 (mTORC1) and mTOR complex 2 (mTORC2). mTORC1 is a key mediator of translation and cell growth, via its substrates p70S6 kinase (p70S6K) and eIF4E binding protein 1 (4E-BP1), and promotes cell survival via the serum and glucocorticoid-activated kinase (SGK), whereas mTORC2 promotes activation of prosurvival kinase AKT.[5−8] mTORC1, but not mTORC2, can be inhibited by an intracellular complex between rapamycin and FK506 binding protein (FKBP).[9,10] However, rapamycin−FKBP may indirectly inhibit mTORC2 in some cells by sequestering mTOR protein and thereby inhibiting assembly of mTORC2.[11]

Given the role of mTOR signaling in cellular growth, proliferation, and survival as well as its frequent deregulation in cancers, several rapamycin analogues (rapalogues) that are selective allosteric mTORC1 inhibitors have been extensively evaluated in a number of cancer clinical trials. Demonstrated clinical efficacy for rapalogues is currently limited to patients with advanced, metastatic renal cell carcinoma (RCC) despite extensive development efforts. This result is likely attributed not only to a lack of inhibition of mTORC2 by rapalogues that leads to upregulation of Akt through a negative feedback loop, but also to only partial inhibition of mTORC1.[12,13] Therefore, ATP-competitive mTOR inhibitors that should simultaneously inhibit both mTORC1 and mTORC2 may offer a clinical advantage over rapalogues.

As a key component of the phosphoinositide 3-kinase-related kinase (PIKK) family, which is comprised of phosphoinositide 3-kinases (PI3Ks), DNA-PK, ATM, and ATR, mTOR shares the highly conserved ATP binding pockets of the PI3K family with sequence similarity of 25% in the kinase catalytic domain.[14] In light of this fact, it is not surprising that many of the first reported ATP-competitive mTOR inhibitors such as BEZ235 and GDC-0980 (Figure 1) also inhibited PI3Ks.[15−18] PI3Ks are responsible for the production of 3-phosphoinositide lipid second messengers such as phosphatidylinositol 3,4,5-triphosphate (PIP3), which are involved in a number of critical cellular processes, including cell proliferation, cell survival, angiogenesis, cell adhesion, and insulin signaling. Therefore, the development of ATP-competitive mTOR inhibitors that are selective over PI3Ks may offer an improved therapeutic potential relative to rapalogues as well as dual PI3K/mTOR inhibitors. Recently, several selective ATP-competitive mTOR inhibitors such as Torin 2 and AZD8055 (Figure 1) have been reported with sufficient promise to warrant clinical trials.[11,19−26] Herein we describe the identification, characterization, and lead optimization of a structurally novel class of mTOR inhibitors exemplified by compound **28**, derived from a benzoxazepine scaffold.

Received: June 6, 2012

   dx.doi.org/10.1021/jm3007933 | *J. Med. Chem.* XXXX, XXX, XXX−XXX

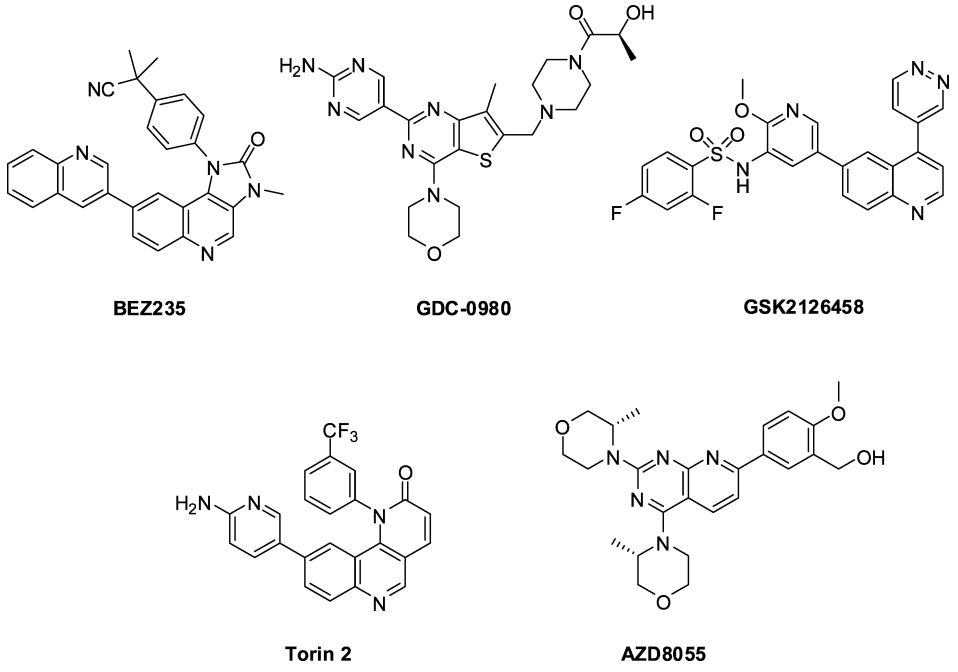

Figure 1. Literature examples of dual PI3K/mTOR and selective ATP-competitive mTOR inhibitors.

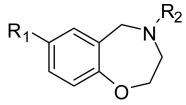

Compound	R_1	R_2	mTOR IC_{50} (nM)[1]	PI3Kα IC_{50} (nM)[1]
1	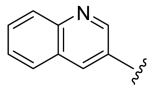	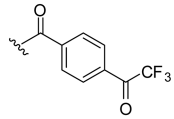	95	398
1a	H	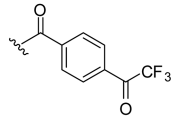	>10,000	>10,000
1b	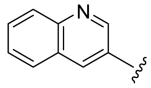	H	>10,000	>10,000
1c	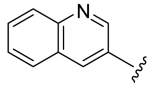	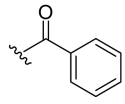	200	3128

Figure 2. Early benzoxazepine derivatives of HTS hit **1**. Note 1: average IC_{50} ($n \geq 2$).

RESULTS AND DISCUSSION

Efforts directed toward the identification of mTOR-selective inhibitors were initiated by high-throughput screening (HTS) of our in-house compound library against mTOR. The measurement of mTOR activity was performed in an ELISA assay format following the phosphorylation of 4E-BP1 protein in a 384-well format. We found a number of potential candidates suitable for lead optimization studies, but one that we found to be particularly attractive was benzoxazepine **1** (Figure 2). It was a potent inhibitor of mTOR (IC_{50} = 95 nM) with 4-fold selectivity over PI3Kα (IC_{50} = 398 nM) and much more pronounced selectivity over other kinases in a preliminary screen. With a molecular weight below 500, a cLogP below 5, a topological polar surface area below 60 Å^2, five rotatable bonds, four hydrogen bond acceptors, and no hydrogen bond donors, it falls within traditionally desirable druglike parameters. Given these characteristics, we were therefore surprised that the benzoxazepine scaffold has received relatively little attention in drug discovery.

While reconfirming the activity of our initial lead, we also performed a rapid assessment of simple perturbations around the benzoxazepine scaffold which suggested that both substituents were critical. Analogues lacking the quinoline at the 7-position (**1a**) and the 4-ketobenzamide at the 4-position (**1b**) displayed none of the activity of the original lead. Simplified benzamide **1c**, however, was only slightly less potent than **1**

dx.doi.org/10.1021/jm3007933 | J. Med. Chem. XXXX, XXX, XXX−XXX

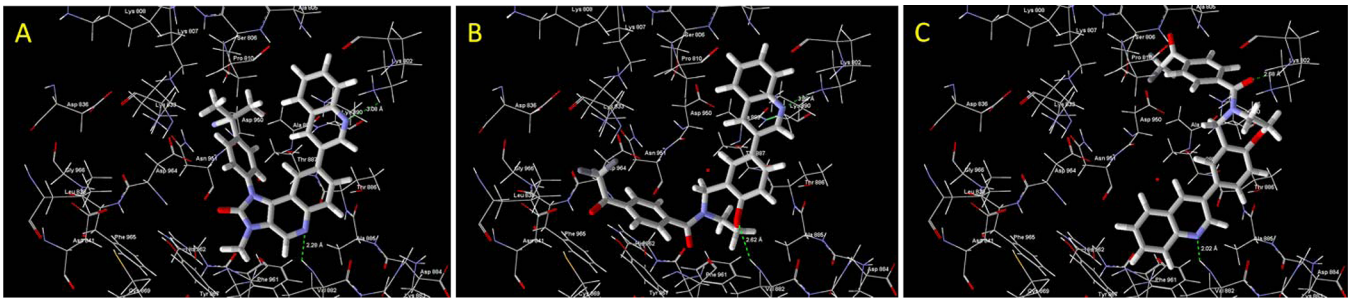

Figure 3. (A) Proposed binding orientation of BEZ235 in PI3Kγ (PDB code 1E8Z).[27] (B) Potential binding orientation of **1** where benzoxazepine oxygen forms a hinge region hydrogen bond. (C) Potential binding orientation of **1** where quinoline nitrogen forms a hinge region hydrogen bond.

with modestly improved selectivity over PI3Kα. This provided us with some confidence that further optimization was possible.

While we were encouraged by the potential of **1** as an initial candidate, it was unclear exactly how it was interacting with the target, and we did not have crystallographic mTOR assets to provide any insight. An examination of how compounds such as BEZ235 interact with the structurally similar PI3K suggested a critical hydrogen bond between the core imidazoquinoline ring and the hinge region valine and provided a schematic model for the binding pocket (Figure 3).[27] One possible binding orientation for **1** involved the quinoline interacting in a similar fashion to form a hydrogen bond at the same site. Alternatively, the ring oxygen of the benzoxazepine core could be envisioned to perform this function. The latter possibility represents a binding orientation that has never been described, but seemed plausible in light of the numerous morpholine oxygens such as in GDC-0980 that have been reported to play a similar role.[18]

Furthermore, even though we were intrigued by the promising characteristics of **1**, we knew that there was plenty of room for improvement. In addition to increasing potency and selectivity, we needed to find analogues with cellular activity and improved ADME (absorption, distribution, metabolism, and excretion) properties such as poor mouse liver microsome stability (23% remained after 30 min), moderate kinetic solubility (K_{sol} = 40.1 μM), and poor cell permeability (Madin−Darby canine kidney (MDCK) P_{app} = 16.9 nm/s). Toward that end, in vitro cellular activity was examined by assessing inhibition of phosphorylation of pS6 (S240/244), a downstream protein in mTORC1 signaling, in a PC-3 cell line.[28] Inhibition of growth-factor-stimulated phosphorylation of AKT (S473), a downstream protein in mTORC2 signaling, was also determined in the same cell line for compounds with >100-fold selectivity and >200 nM IC_{50} against PI3Kα.

We initiated our structure−activity relationship (SAR) efforts with the goal in mind of determining which of the two likely binding orientations was responsible for our activity. Naphthalene derivative **2** rapidly provided the answer (Table 1). Retention of the mTOR activity of **2** effectively ruled out the potential binding orientation depicted in Figure 3C and prompted us to focus our attention on the prospects of the novel binding orientation in Figure 3B. Furthermore, this simple change afforded a substantial improvement in the selectivity for mTOR activity over PI3Kα, and even the simple phenyl substituent **3** was reasonably active. Addition of polar functionality has a dramatic impact on activity, especially when appended in a slightly extended orientation. For example, installation of an acetamide such as in **5** leads to a substantial increase in activity against PI3Kα with virtually no impact on mTOR activity. The more constrained indazole group provided analogues with significantly greater mTOR activity and restored selectivity over PI3Kα. We were also gratified to note that both indazole analogues **6** and **7** exhibited submicromolar cellular activity as well. The impact of functionality capable of serving as a proton donor appears to be substantial, as methylated analogue **9** leads to a >20-fold loss in potency versus desmethyl derivative **8**. Additionally, the drop in activity of the truncated pyrazole analogue **10** demonstrated the value of the phenyl "spacer". The best group found from these initial efforts was the benzimidazole (**11** and **12**), with **12** being the most potent in our biochemical assay thus far. In fact, **12** was the first subnanomolar mTOR inhibitor we found with greater than 100-fold selectivity over PI3Kα. The benzimidazole was a particularly intriguing alternative, as the tautomeric nature allows for multiple orientations that could serve as a proton donor. We were pleased to note a corresponding increase in cellular potency for the benzimidazoles. In addition, both **11** and **12** showed comparable stability in a mouse liver microsome stability study with approximately 50% of both compounds remaining after 30 min. These data translated to similar mouse plasma exposure levels of both **11** (1.5 μM at 1 h and 0.4 μM at 4 h) and **12** (1.0 μM at 1 h and 0.2 μM at 4 h) when dosed orally at 100 mg/kg. We considered **11** to be slightly superior to **12** due to increased cellular potency and higher oral exposure in mouse. However, **11** suffered from poor ADME characteristics such as low kinetic solubility (K_{sol} < 1.0 μM), poor cell permeability (MDCK P_{app} = 9.8 nm/s), and inhibition of <3 μM against CYP 2C9 and 3A4 isoforms. Additionally, we were interested in compounds with a greater level of selectivity against PI3Kα.

In light of the evidence that suggested the binding orientation depicted in Figure 3B, we were reasonably confident that substitution at any other position around the aromatic portion of the benzoxazepine core would interfere with mTOR binding. All attempts to explore even the simplest analogues led to a complete loss of activity and were quickly abandoned. We therefore turned our attention to exploring substitution about the oxazepine ring.

We anticipated that the trifluoromethyl ketone functionality on our initial hit represented an opportunity for optimization of the ADME characteristics. We therefore prepared a number of amide derivatives using the benzimidazole as a standard substituent. Given the dramatic drop in activity we observed in our initial SAR efforts when we removed the para substituent, we decided to focus on those derivatives. We were pleased to discover that a variety of substituents were well tolerated (Table 2) with respect to mTOR activity. Extrusion of the ketone carbonyl group (**13**) significantly improved mTOR

dx.doi.org/10.1021/jm3007933 | J. Med. Chem. XXXX, XXX, XXX−XXX

Table 1. mTOR Activity, PI3Kα Activity, Cellular Activity, MLM, and CYP Inhibition Data for Right-Hand-Side Modifications of 1[a]

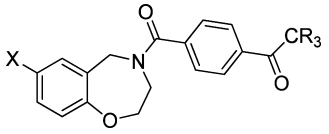

Compound	X	R	mTOR IC_{50} (nM)[1]	PI3Kα IC_{50} (nM)[1]	Cell[2] IC_{50} (nM)[1]	MLM[1,3]
1	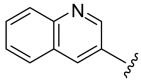	F	95	398	n.d.[4]	n.d.
2	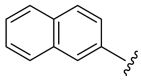	F	73.7	1463	n.d.	n.d.
3		F	119	2305	n.d.	n.d.
4		F	72.7	1131	n.d.	n.d.
5	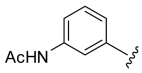	F	115	238	n.d.	n.d.
6	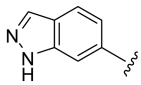	F	3.5	259	674	60
7	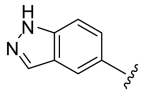	F	4.3	137	503	23
8	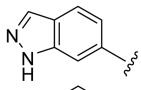	H	14	1800	n.d.	n.d.
9	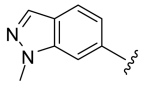	H	342	2447	n.d.	n.d.
10	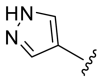	F	29.7	1048	718	3
11	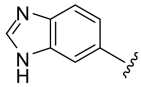	F	2.3	89	151	49
12	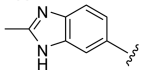	F	0.5	89	239	50

[a]Notes: (1) average IC_{50} ($n \geq 2$); (2) pS6 (S240/244) in PC-3; (3) percent remaining after 30 min; (4) Not determined.

Table 2. mTOR Activity, PI3Kα Activity, Cellular Activity, MLM, and CYP Inhibition Data for Right-Hand-Side Modifications of 11

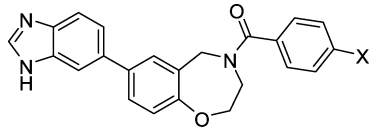

						CYP inhibition (μM)			
compd	X	mTOR IC_{50}[a] (nM)	PI3Kα IC_{50}[a] (nM)	cell[b] IC_{50}[a] (nM)	MLM[c]	2C8	2C9	2D6	3A4
11	$COCF_3$	2.3	89	151/–	49	6.2	0.8	4.0	2.3
13	CF_3	3.5	1092	306/680	74	3.6	1.6	3.1	1.9
14	SO_2NH_2	2.9	763	1801/1672	64	13.9	1.3	4.3	6.3
15	SO_2NHMe	3.5	1090	451/812	64	1.6	1.1	2.3	2.8
16	SO_2Me	4.4	670	342/805	82	>20	3.0	8.1	3.8
17	SO_2Et	3.6	2172	343/1077	72	5.0	1.7	3.3	2.2

[a]Average IC_{50} ($n \geq 2$). [b]pS6 (S240/244)/pAKT (S473) in PC-3. [c]Percent remaining after 30 min.

dx.doi.org/10.1021/jm3007933 | J. Med. Chem. XXXX, XXX, XXX−XXX

Table 3. mTOR Activity, PI3Kα Activity, Cellular Activity, MLM, and CYP Inhibition Data of Substituted Modifications of 16

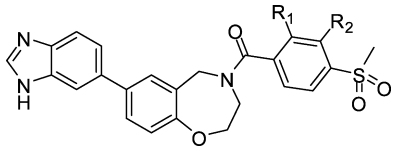

compd	R_1	R_2	mTOR IC_{50}[a] (nM)	PI3Kα IC_{50}[a] (nM)	cell[b] IC_{50}[a] (nM)	MLM[c]	CYP inhibition (μM) 2C8	2C9	2D6	3A4
16	H	H	4.4	670	343/805	82	>20	3.0	8.1	3.8
18	Me	H	5.7	>3000	422/1007	51	5.4	2.9	9.3	4.1
19	Et	H	5.2	>3000	233/689	50	5.6	5.4	>20	2.0
20	n-Pr	H	28.0	>3000	1184/3302	87	nd[d]	nd	nd	nd
21	NHEt	H	204	>3000	nd/nd	nd	nd	nd	nd	nd
22	Cl	H	23.2	705	337/1062	58	5.4	9.0	9.2	3.5
23	Br	H	5.2	693	343/453	45	3.4	4.2	9.2	3.0
24	H	Me	6.6	459	591/1219	68	nd	nd	nd	nd
25	Me	F	1.4	2344	329/437	94	3.4	6.4	9.6	3.4
26	Et	F	2.9	>3000	152/277	59	3.1	2.2	11.5	2.6

[a]Average IC_{50} ($n \geq 2$). [b]pS6 (S240/244)/pAKT (S473) in PC-3. [c]Percent remaining after 30 min. [d]Not determined.

selectivity over PI3Kα without any substantial loss of activity in our primary assays. In addition, this simple change conveyed some stability upon exposure to mouse liver microsomes, although it did not improve upon the CYP inhibition of **11**. A number of analogues were identified that demonstrated >100-fold selectivity for mTOR over PI3Kα, which allowed us to focus on those with improved ADME profiles. Sulfonamides **14** and **15**, for example, suggested that the poor permeability (MDCK P_{app} = 42 nm/s) of the former correlated well with a lack of cellular activity. Among the best of these initial congeners were the alkyl sulfones. Methyl sulfone **16** presented an improvement in CYP inhibition and mouse liver microsome stability compared to **11** and exhibited significantly higher mouse plasma exposure (7.8 μM (at 1 h) and 1.0 μM (at 4 h)) when dosed orally at 100 mg/kg. We felt that these attributes made **16** more attractive than ethyl sulfone **17** despite the increased mTOR selectivity of the latter compound.

Using the methyl sulfone as a reference, we initiated an exploration of additional substitution around the benzamide ring. The introduction of small alkyl groups ortho to the carbonyl such as in **18** and **19** conferred additional selectivity for mTOR over PI3Kα (Table 3). The erosion of activity of *n*-propyl derivative **20** suggests a spatial limitation to perturbations at this position, and the more significant loss of activity of the isosteric **21** infers that the potential internal hydrogen bond between the NH and the carbonyl is not favored. Other types of ortho substituents such as the halogenated analogues **22** and **23** were tolerated, but did not lead to any discernible improvement. Likewise, monosubstitution at the position ortho to the sulfonyl group such as in **24** failed to impart any benefit over **16**. However, substitution at both positions proved beneficial. For example, fluorinated analogues **25** and **26** are both more than 1000-fold selective for mTOR over PI3Kα. Additionally, the mouse liver microsome stability of **25** was particularly attractive, as >90% remained after incubation for 30 min.

Equipped with an improved amide alternative, we revisited the benzimidazole standard with the intent of improving the CYP inhibition profile. After extensive evaluation, the aminopyridine proved to be the best alternative. Comparison of **16** with **27** (Table 4) shows that the CYP and mouse liver microsome profile for the aminopyridine analogue is a considerable improvement over that of the original benzimidazole, even though that improvement comes with approximately a 3-fold loss in potency. We reasoned that the use of the optimized amide would restore some of that lost activity, which was confirmed by comparison of benzimidazole **25** to aminopyridine **28** (XL388).[29] It should be noted at this point that our biochemical assay proved to be reasonably robust. Over the course of 35 different IC_{50} determinations for **28**, we observed a range between 14.7 and 4.3 nM with a standard deviation of 2.8. We were delighted to see that **28** was not only very active and selective in our biochemical and cellular assays, but exhibited an attractive in vitro ADME and physicochemical profile. Our initial screen of CYP isoform inhibition did not reveal significant inhibition below a concentration of 10 μM, but did reveal a reasonable mouse liver microsome stability of 75% after incubation for 30 min along with acceptable permeability (MDCK P_{app} = 151 nm/s) and kinetic solubility (K_{sol} = 232 μM).

In light of the promising in vitro characteristics of **28**, we undertook an investigation of its in vivo parameters. The mean plasma protein binding of **28** in human, monkey, dog, rat, and mouse plasma was evaluated at 5 μM and was determined to be 86%, 90%, 89%, 85%, and 84%, respectively, suggesting a significant free concentration of **28** in the plasma. An initial examination in a mouse study revealed substantial and sustained plasma exposure (22.0 μM at 1 h and 17.8 μM at 4 h) following an oral dose at 100 mg/kg. Further examination of the liver microsomal stability of **28** in a mammalian panel revealed that 93%, 65%, 82%, and 78% for human, monkey, dog, and rat, respectively remained after 30 min. Gratifyingly, this promising stability data translated to reasonable oral exposure in expanded pharmacokinetic studies (Table 5). The dog pharmacokinetic profile of **28** dosed as a solution at 3 mg/kg is shown in Figure 4.

To ascertain the mode of inhibition of mTOR by **28**, we determined the IC_{50} values at varying ATP concentrations.[30] These results revealed that **28** acts in an ATP-competitive manner, with a linear increase in IC_{50} values with increasing ATP concentration (Figure 5). Additionally, **28** demonstrated rapidly reversible inhibition of mTOR activity. A solution of

dx.doi.org/10.1021/jm3007933 | J. Med. Chem. XXXX, XXX, XXX−XXX

Table 4. Summarized Data of Advanced Compounds[a]

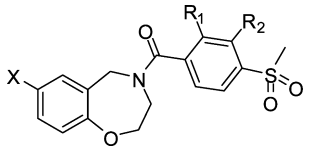

Compound	X	R_1	R_2	mTOR IC_{50} (nM)[1]	PI3Kα IC_{50} (nM)[1]	Cell[2] IC_{50} (nM)[1]	MLM[3]	CYP Inhibition (μM)			
								2C8	2C9	2D6	3A4
16	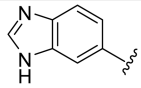	H	H	4.4	670	343/805	82	>20	3.0	8.1	3.8
25	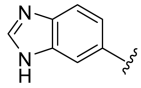	Me	F	1.4	2344	329/437	94	3.4	6.4	9.6	3.4
27	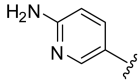	H	H	13	2895	1179/1969	100	>20	18.8	>20	>20
28 (XL388)	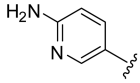	Me	F	9.9	>3,000	273/330	78	>20	10.6	>20	24.6

[a]Notes: (1) average IC_{50} ($n \geq 2$); (2) pS6 (S240/244)/pAKT (S473) in PC-3; (3) percent remaining after 30 min.

Table 5. PK Properties of 28

species	C_{max}, iv/po	T_{max}, po	$AUC_{0-\infty}$ (μM·h), iv/po	$T_{1/2}$ (h), iv	CL (L/kg/h), iv	V_{ss} (L/kg), iv	F (%), po
mouse[a] (10 mg/kg)	9.14/1.30	0.5	8.00/2.51	1.35	2.75	1.96	31.4
rat[a] (3 mg/kg)	4.12/0.707	0.5	3.72/0.952	0.45	1.27	1.27	25.6
dog[a] (3 mg/kg)	2.28/1.66	1.0	11.0/7.66	6.11	0.598	3.15	69.6
cyno[b] (3 mg/kg)	0.95/0.25	2.0	1.31/0.70	0.86	5.05	6.42	53.4

[a]Formulation EPW (5% EtOH/45% PEG400/water + 1:2 HCl (m/m). [b]Formulation EPW (5% EtOH/45% PEG400/water + 1:1.5 HCl (m/m).

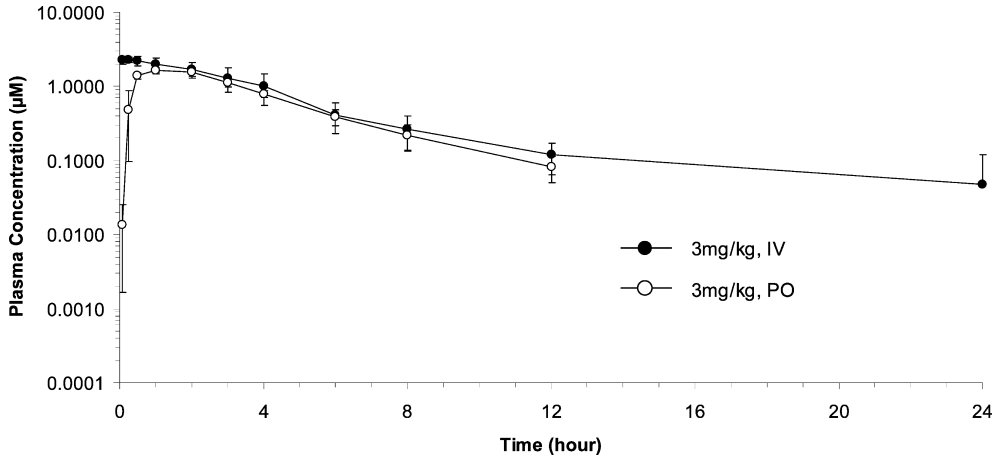

Figure 4. Pharmacokinetic profile of **28** in dogs. Compound **28** was dosed at 3 mg/kg in male beagles. Data are reported as the mean ± SD (n = 3).

mTOR saturated with **28** was diluted with a mixture containing 1 mM ATP, revealing rapid and complete recovery of enzyme activity ($t_{1/2}$ < 2 min) compared to an enzyme control in the absence of inhibitor. In addition, **28** showed no cross-reactivity (<3000 nM) with members of the PI3KK lipid kinase superfamily as well as a panel of 141 protein kinases tested in house or by Millipore (Table 6). The hERG (manual Patchclamp, 15.9 μM), P-glycoprotein (>20 μM), and PXP CYP3A4 induction (50 μM) of **28** was also characterized. Collectively, the attractive in vitro and in vivo ADME profile along with high mTOR biochemical and cell potency of **28** provided validation that it could serve as a viable selective and ATP-competitive mTOR inhibitor.

To assess the pharmacodynamic effects of our inhibitor on the mTOR pathway signaling, athymic nude mice bearing PC-3

dx.doi.org/10.1021/jm3007933 | J. Med. Chem. XXXX, XXX, XXX−XXX

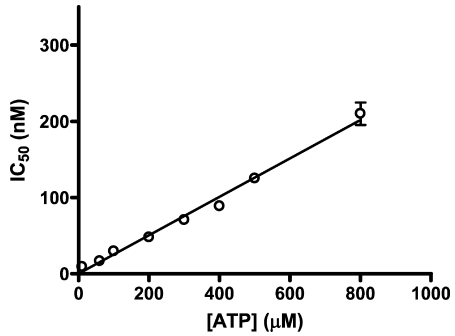

Figure 5. IC_{50} for **28** as a function of the ATP concentration. Error bars represent the standard error of the mean on four IC_{50} values at each ATP concentration.

prostate tumors were dosed orally at 100 mg/kg of **28**. Rapamycin was also administered intraperitoneally at 5 mg/kg as a reference. Plasma and tumor samples were collected at 1, 4, 8, 16, 24, and 32 h for **28** and at 4 h for rapamycin after dosing and homogenized with buffer. Tumor lysates from each animal (n = 5) were then pooled for each group and analyzed by immunoblot for levels of phosphorylated p70S6K, S6, 4E-BP1, and AKT. Strong inhibition of both mTORC1 readout (p-p70S6K, p-S6, p-4E-BP1) and mTORC2 readout (p-AKT (S473)) was achieved 4−8 h following administration of **28**, which diminished to near-basal levels of phosphorylation by 16 h postdose (Figure 6). Modest inhibition (39−45%) of phosphorylation of the PI3K target AKT (T308) was also observed 4−8 h postdose, returning to basal levels of phosphorylation by 16 h postdose. Rapamycin resulted in strong inhition of the mTORC1 biomarkers but had no effect on the mTORC2 biomarker as expected. Similar levels of pharmacodynamic effects of **28** on the mTOR signaling pathway were also observed in athymic nude mice bearing MCF-7 xenograft tumors when dosed orally at 100 mg/kg.[31] Maximal inhibition (85−96%) of phosphorylation of mTORC1 readout (p70S6K, S6, 4E-BP1) as well as mTORC2 readout (AKT (S473)) was achieved 1 h following administration of **28** and was sustained through 8 h postdose (Figure 7). Significantly, moderate to strong

Table 6. Kinase Profile of 28

kinase	IC_{50}[a] (nM)
PI3Kα	>3000[b,c]
PI3Kβ	>5000[b,c]
PI3Kγ	>5000[b,c]
PI3Kδ	>5000[b,c]
DNA-PK	8831[b]
VPS34	>3500[b,c]
AKT1; ALK; CDC7; CHK1; cRAF1; EGFR; ERBB2; FAK; FLT1; FLT3; HSP90; IRK; JAK2; KDR; KIT; MEK1; MET; p70S6K; PDGFRβ; PDK1; PIM1; SRC	>3500[b,c]
EPH4; FGFR1; FGFR2; FGFR3; FGFR4; IPFK2; RSK2	>10000[b,c]
ABL; ACK1; ARG; AMPK; ASK1; AKT2; AKT3; Aurora-A; AXL; BLK; BRK; BRSK1; CaMKI; CaMKIV; CDK3/CyclinE; CDK5/p25; CHK2; CK1δ; CK2; CLK2; CSK; DAPK2; DDR2; DYRK2; EPHA2; EPHB1; FES; GCK; GRK5; GSK3α; GSK3β; Haspin; HCK; HIPK2; IGF-1R; IKKα; IKKβ; IRAK1; ITK; JNK1α1; JNK2α2; JNK3; LIMK1; LKB1; LOK; LYN; MAPK1; MAPK2; MAPKAP-K3; MARK1; MER; MINK; MKK4; MKK6; MKK7β; MLK1; MNK2; MSK1; MSSK1; MST1; MuSK; NEK2; NEK7; NLK; PAK3; PAK6; PASK; PDK1; PKA; PKCα; PKCβI; PKCβII; PKCγ; PKCδ; PKCε; PKCη; PKCι; PKCμ; PKCθ; PKCζ; PKD2; PKG1β; PLK1; PLK3; PRAK; PRK2; PYK2; RET; RIPK2; ROCK-I; ROCK-II; ROS; RSE; RSK1; RSK3; RSK4; SGK; SGK2; SGK3; STK33; TAK1; TAO1; TBK1; TSSK1; ULK2; WNK2; VRK2; YES; ZAP-70; ZIPK	>10000[b,d]

[a]Average IC_{50} ($n \geq 2$). [b]Kinases tested in house. [c]Highest concentration tested. [d]Kinases tested by Millipore (Charlottesville, VA).

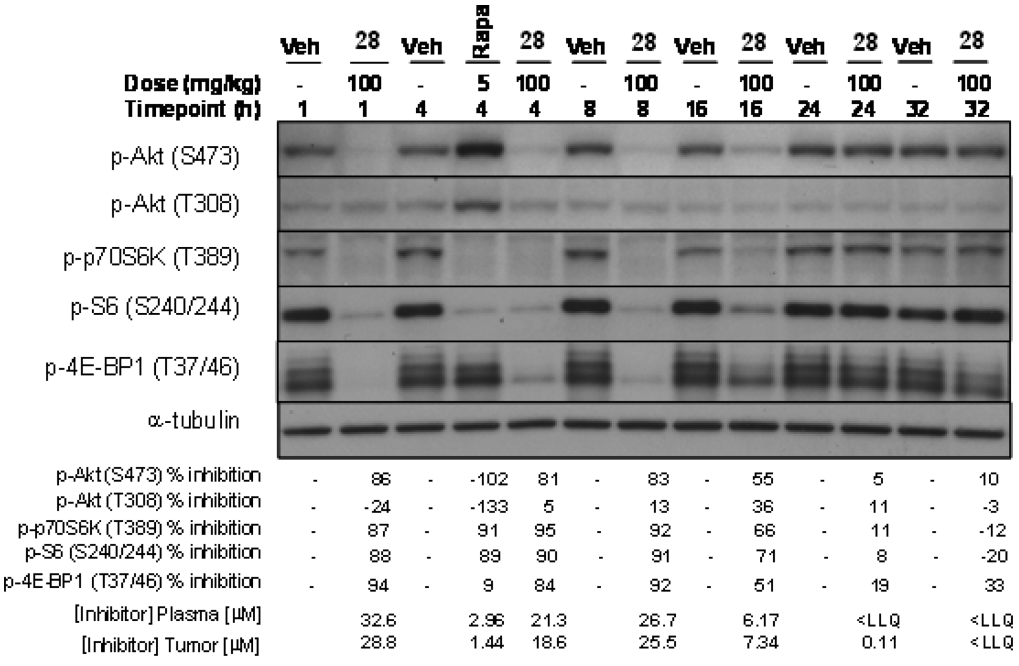

Figure 6. Inhibition (%) of phosphorylation of p70S6K, S6, 4E-BP1, and AKT in PC-3 xenograft tumors and exposure data after a single oral dose (100 mg/kg).

dx.doi.org/10.1021/jm3007933 | J. Med. Chem. XXXX, XXX, XXX−XXX

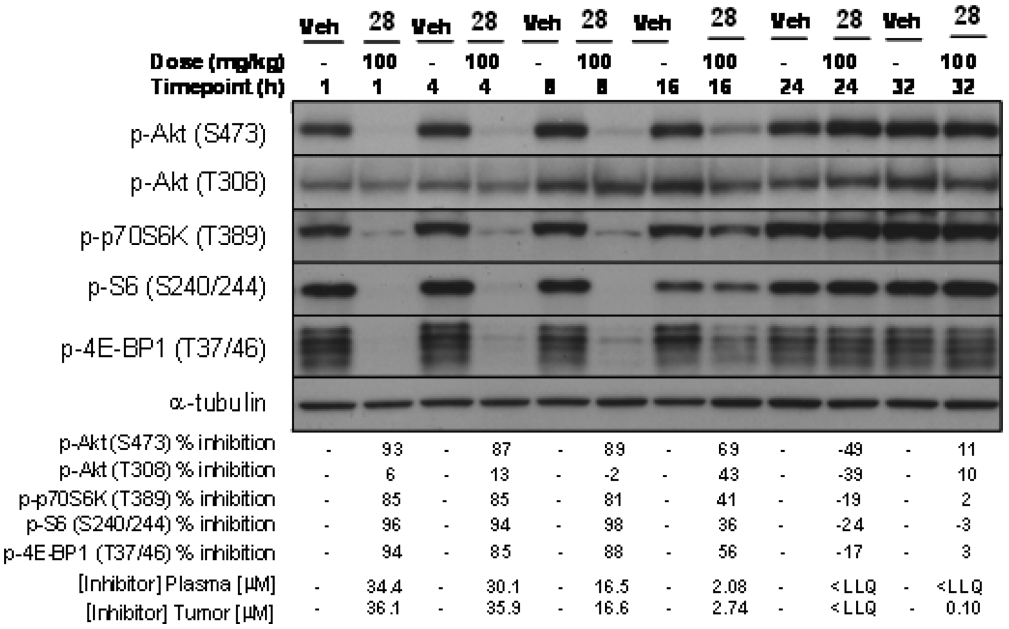

Figure 7. Inhibition (%) of phosphorylation of p70S6K, S6, 4E-BP1, and AKT in MCF-7 xenograft tumors and exposure data after a single oral dose (100 mg/kg).

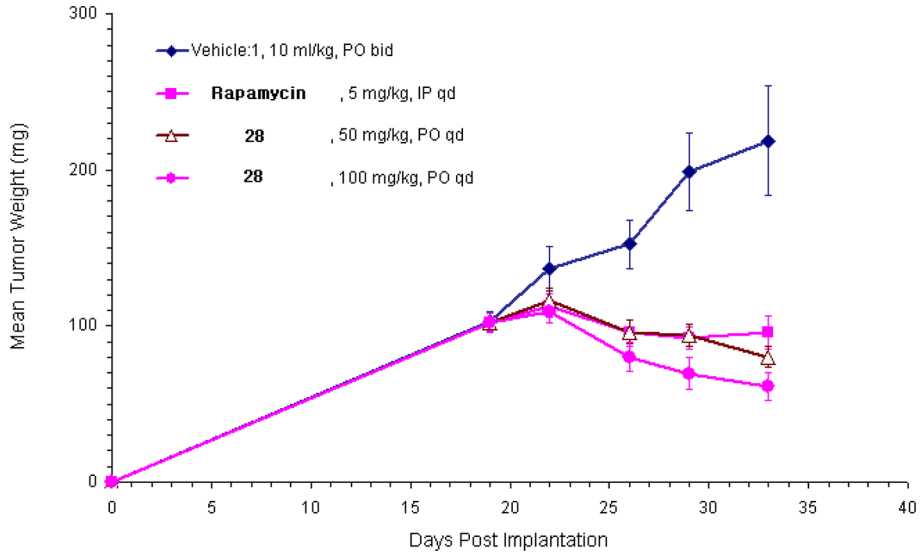

Figure 8. In vivo efficacy of **28** in MCF-7 xenograft tumors.

(36–69%) inhibition of phosphorylation was still observed through 16 h postdose before returning to basal levels by the 24 h time point.

Having identified a potent and selective inhibitor of mTOR with strong pharmacodynamic effects and good mouse oral exposure, we decided to assess its antitumor efficacy. Specifically, **28** was administered to animals implanted with MCF-7 xenograft tumors to determine its effects on tumor growth. Rapamycin was used as a control to compare the results to those of a selective mTORC1 inhibitor. Tumors were established in female athymic nude mice and staged when the average tumor mass reached 102 ± 17.7 mg. Compound **28** was orally administered as a solution/fine suspension in water (with 1:1 molar ratio of HCl) once daily (qd) at 50 and 100 mg/kg for 14 days. Rapamycin, formulated at 5 mg/kg in 12.5 ethanol, 12.5 cremophor, and 75% Hank's balanced salt solution (HBSS), was administered intraperitoneally (ip) once daily also for 14 days. Compound **28** resulted in complete inhibition of MCF-7 xenograft tumor growth at both doses (Figure 8), with significant tumor regression of 22% and 40% below pretreatment values at the 50 and 100 mg/kg doses, respectively. Furthermore, **28** does not appear to show significant toxicity. Mice in the 50 mg/kg cohort over the course of the study gained on average 2.2% additional mass, while those in the 100 mg/kg cohort lost on average 2.8% of their body mass. These results correlate well with the pharmacodynamic activity of **28** and taken in conjunction with its inhibition of cell proliferation (proliferation IC_{50} = 1.37 μM in MCF-7 cell line) suggest that blockade of mTOR signaling is a viable target for antitumor activity. Rapamycin also resulted in complete inhibition of tumor growth, although significant tumor regression below pretreatment values was not achieved at 5 mg/kg.

dx.doi.org/10.1021/jm3007933 | J. Med. Chem. XXXX, XXX, XXX–XXX

CHEMISTRY

We recognized from the outset that benzoxazepine **29** was going to be a critical synthetic intermediate in this project. While we initially accessed this compound via the previously reported synthesis,[32] subsequently a new synthetic route was designed which was more amendable to a larger scale preparation of the intermediate in Scheme 1. We envisioned that the benzoxazepine core could be accessible from intermediate **30**, which could be generated from commercially available 5-bromosalicylaldehyde. Reductive amination of 5-bromosalicylaldehyde with 2-aminoethanol followed by Boc protection provided **30**, which was then converted to benzoxazepine **29** through a Mitsunobu reaction. Particularly noteworthy about this new route is that we could routinely prepare over 200 g of benzoxazepine **29** in a single batch. Metal–halogen exchange of **29** with *n*-BuLi at −78 °C in the presence of triisopropoxyborate afforded benzoxazepinylboronic acid **31**, another useful synthetic intermediate.

Scheme 1[a]

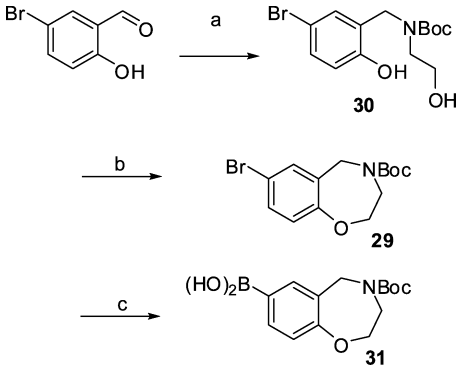

[a]Reagents and conditions: (a) 2-aminoethanol, $NaBH_4$, MeOH, Boc_2O; (b) $(Ph)_3P$, DIAD, THF, (c) *n*-BuLi, THF, triisopropyl borate, −78 °C, HCl.

We also required a synthetic route that would provide access to noncommercially available 4-(methylsulfonyl)benzoic acid derivatives. Toward that end, treatment of 2-bromo-4-(methylsulfonyl)benzoic acid[33] with (trimethylsilyl)diazomethane in THF/MeOH afforded methyl 2-bromo-4-(methylsulfonyl)-benzoate (**32**) (Scheme 2). Silver-promoted Suzuki–Miyaura coupling of **32** with ethylboronic acid followed by hydrolysis provided benzoic acid **33**.[34] In a similar manner, *n*-propyl derivative **33** was prepared. Buchwald–Hartwig amination of **32** with ethylamine in the presence of xantphos gave the corresponding anthranilate,[35] which was hydrolyzed to yield acid **35**.

The synthesis of tetrasubstituted carboxylate **37** began with bromination of 2,3-difluorotoluene followed by selective metal–halogen exchange of the bromide and trapping with CO_2 to give acid **36** (Scheme 3). Selective displacement of the fluoride para to the carboxylate with sodium thiomethoxide and subsequent oxidation with Oxone afforded 3-fluoro-2-methyl-4-(methylsulfonyl)benzoic acid (**37**). A similar approach was used for the preparation of ethyl derivative **39**, but we required a convenient source of the requisite 2,3-difluoroethylbenzene. Borane reduction of the corresponding commercially available acetic acid produced the anticipated primary alcohol (Scheme 4), which was efficiently converted to **38** via tosylation, bromination, and reductive dehalogenation. With the appropriate ethyl starting material in hand, acid **39** was generated without incident following the previously developed protocol.

Scheme 3[a]

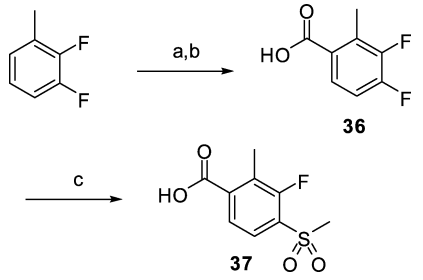

[a]Reagents and conditions: (a) Fe, Br_2, $CHCl_3$; (b) $^{i}PrMgCl$, THF, CO_2; (c) $NaSCH_3$, DMF, Oxone, NaOH, $NaHCO_3$, acetone/H_2O (1:1), 0 °C.

Our plan from the outset was to install the left-hand-side functionality via a Suzuki–Miyaura coupling. For coupling partners where the desired boronic acid was commercially

Scheme 2[a]

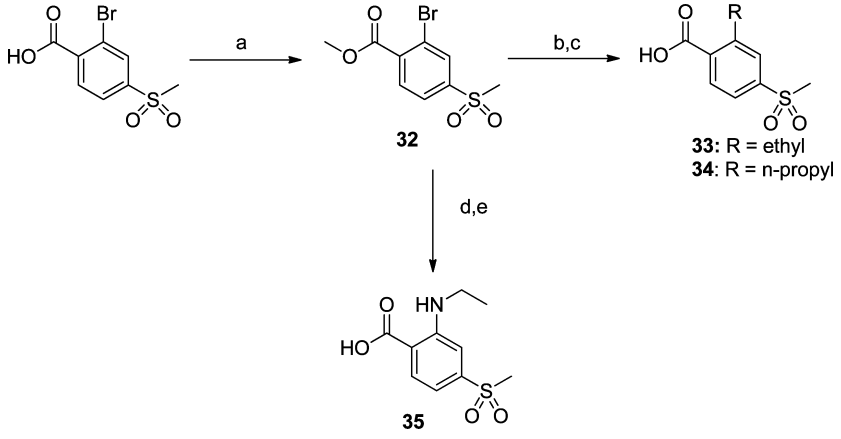

[a]Reagents and conditions: (a) $(TMS)CHN_2$, THF/MeOH (2:1), 0 °C; (b) $RB(OH)_2$, [1,1′-bis(diphenylphosphino)ferrocene]dichloropalladium-(II) complex with dichloromethane, K_2CO_3, Ag_2O, THF, 85 °C; (c) MeOH, 1 N NaOH, 45 °C; (d) ethylamine, $Pd_2(dba)_3$, xantphos, Cs_2CO_3, 1,4-dioxane, 95 °C; (e) CH_2Cl_2/MeOH (1:1), 1 N NaOH, 45 °C.

dx.doi.org/10.1021/jm3007933 | J. Med. Chem. XXXX, XXX, XXX–XXX

Scheme 4[a]

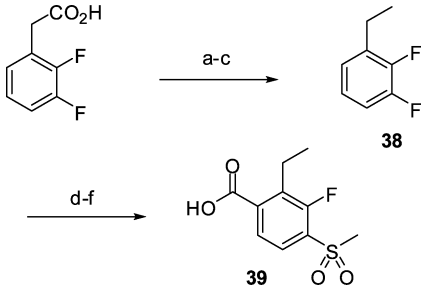

[a]Reagents and conditions: (a) BH_3−SMe_2, THF; (b) TsCl, Et_3N, CH_2Cl_2, LiBr, acetone; (c) Mg, Et_2O, $BrCH_2CH_2Br$, aqueous NH_4Cl; (d) Fe, Br_2, $CHCl_3$; (e) ^iPrMgCl, THF, CO_2; (f) $NaSCH_3$, DMF, Oxone, NaOH, $NaHCO_3$, acetone/H_2O (1:1), 0 °C.

available, direct coupling with bromide **29** formed the desired carbon−carbon bond such as for **40** in Scheme 5. Standard Boc

Scheme 5[a]

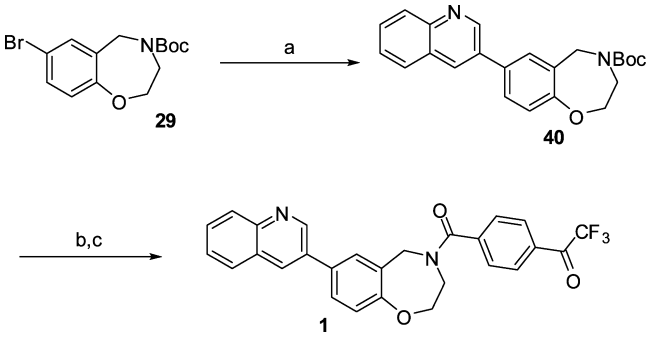

[a]Reagents and conditions: (a) quinolin-3-ylboronic acid, [1,1′-bis(diphenylphosphino)ferrocene]dichloropalladium(II) complex with dichloromethane, triethylamine, 1,4-dioxane, H_2O, 85 °C; (b) 4 N HCl, 1,4-dioxane, rt; (c) *N*,*N*-diisopropylethylamine, HATU, DMF, 4-(2,2,2-trifluoroacetyl)benzoic acid, rt.

deprotection in acid followed by HATU (*O*-(7-azabenzotriazol-1-yl)-*N*,*N*,*N*′,*N*′-tetramethyluronium hexafluorophosphate) coupling with 4-(2,2,2-trifluoroacetyl)benzoic acid afforded compound **1**. Compounds **1a−c**, **2−5**, and **10** were synthesized in a similar manner. Alternatively, the Suzuki−Miyaura coupling reaction could be performed using the boronic acid of the benzoxazepine previously described. For example, reaction of **31** with 6-bromo-1*H*-indazole smoothly formed the anticipated product **41** (Scheme 6), which was then subjected to the same deprotection/esterification sequence to yield **6**. This latter route was used for the synthesis of **7−9** and **11−28** and was sufficiently scalable that it was used to prepare over 100 g of **28** in a single batch.

In conclusion, a series of structurally novel and highly potent mTOR inhibitors with complete selectivity over the PI3Ks were discovered. Starting from HTS hit **1**, lead optimization efforts on both the left- and right-hand sides of the benzoxazepine core led to the identification of **28**, which inhibits mTOR at low nanomolar concentration while exhibiting exquisite selectivity over a large panel of kinases tested. Compound **28** also exhibited good in vitro multispecies liver microsome stability and showed good oral exposure with moderate to good half-lives in several species. Profound pharmacodynamic effects were observed with **28** in both PC-3 and MCF-7 xenograft

Scheme 6[a]

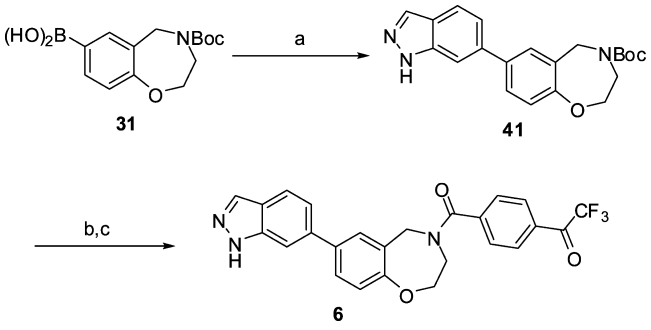

[a]Reagents and conditions: (a) 6-bromo-1*H*-indazole, 1,1′-bis(diphenylphosphino)ferrocene]dichloropalladium(II) complex with dichloromethane, triethylamine, 1,4-dioxane, H_2O, 85 °C; (b) 4 N HCl, 1,4-dioxane, rt; (c) *N*,*N*-diisopropylethylamine, HATU, DMF, 4-(2,2,2-trifluoroacetyl)benzoic acid, rt.

models. Furthermore, an efficacy study in mice bearing MCF-7 xenograft tumors revealed complete tumor growth inhibition. On the basis of these results, compound **28** was selected for drug candidate (DC) status and was subjected to further preclinical evaluation.

EXPERIMENTAL SECTION

All reagents and solvents employed were purchased commercially and used without further purification unless otherwise indicated. Melting points were determined on a Melt-Temp melting point apparatus, model II, and are uncorrected. NMR spectra were recorded on a Varian Mercury Plus 400 MHz instrument. ^{13}C NMR spectra are assigned with peaks "as observed" with no comment on splitting patterns. Reported spectra may appear to contain superfluous signals due to the existence of rotamers and/or carbon−fluorine coupling. Chemical shifts are reported in parts per million relative to an internal standard of tetramethylsilane in deuterated dimethyl sulfoxide (DMSO-d_6), deuterated methanol (CD_3OD), or deuterated chloroform ($CDCl_3$). Positive ion fast atom bombardment (FAB) high-resolution mass spectrometry was conducted by Analytical Instrument Group, Inc., Raleigh, NC. All final compounds were purified to ≥95% purity as assayed by analytical HPLC (YMC-Pack Pro 150 × 4.6 mm, 5 μm C18 column, Shimadzu LC-10AT VP system equipped with a Shimadzu SPD-M10A VP diode array detector) at a 1.5 mL/min flow rate with a gradient of 5−95% acetonitrile (containing 0.1% TFA) in 0.1% aqueous TFA for 25 min and a total run time of 27 min. Pharmacokinetic, liver microsome assay, CYP inhibition, MDCK, and K_{sol} data, reported as average IC_{50} ($n \geq 2$), were carried out as previously described.[36,37]

***tert*-Butyl 7-Bromo-2,3-dihydrobenz[*f*][1,4]oxazepine-4(5*H*)-carboxylate (29).** To a stirred solution of 2-aminoethanol (6.11 g, 100 mmol) in MeOH (60 mL) was added 5-bromosalicylaldehyde (20.1 g, 100 mmol). The reaction mixture was stirred at ambient temperature for 2 h. To this mixture was added sodium borohydride (1.51 g, 40.0 mmol) portionwise with vigorous stirring. After being stirred for an additional 30 min, the reaction mixture was diluted with 6 N NaOH (60 mL). To this mixture was added di-*tert*-butyl dicarbonate (32.7 g, 150 mmol) slowly. After the reaction mixture was stirred for 30 min, an additional amount of di-*tert*-butyl dicarbonate (10.9 g, 50.0 mmol) was added, and the reaction mixture was stirred for an additional 30 min. Most of the methanol was removed on a rotary evaporator, and the residual solid was suspended with H_2O (50 mL). To this suspension was added 1 N HCl slowly with vigorous stirring until the reaction mixture reached pH 4−5. The white precipitates were collected by filtration and washed with H_2O. The precipitates were then suspended with EtOAc (50 mL) and filtered to provide **30** (25.8 g, 75%) as a white solid. MS (EI): *m*/*z* for $C_{14}H_{20}BrNO_4$, found 346.0 (MH^+).

dx.doi.org/10.1021/jm3007933 | J. Med. Chem. XXXX, XXX, XXX−XXX

A stirred solution of **30** (17.3 g, 50.0 mmol) and triphenylphosphine (13.6 g, 52.0 mmol) in THF (100 mL) was cooled to 0 °C, and diisopropyl azodicarboxylate (11.1 g, 55.0 mmol) was added slowly. Upon completion of addition, the reaction mixture was stirred at ambient temperature for 30 min and diluted with H_2O (50 mL) and Et_2O (50 mL). The separated organic layer was washed with 1 N HCl (50 mL), 1 N NaOH (50 mL), and brine, then dried over anhydrous sodium sulfate, and concentrated on a rotary evaporator. The residue was purified with a short silica gel plug (hexanes/ethyl acetate (20:1)) to give **29** (15.2 g, 93%) as a white powder. ^{1}H NMR (400 MHz, $CDCl_3$): δ (rotamers are observed) 7.43−7.27 (m, 2H), 6.93−6.88 (m, 1H), 4.44 and 4.36 (s, 2H), 4.03 and 4.02 (d, J = 4.4 Hz, 2H), 3.79 and 3.78 (d, J = 4.4 Hz, 2H), 1.43 (s, 9H). MS (EI): m/z for $C_{14}H_{18}BrNO_3$, found 328.0 (MH^+).

4-(*tert*-Butoxycarbonyl)-2,3,4,5-tetrahydrobenz[*f*][1,4]-oxazepin-7-ylboronic Acid (31). A stirred solution of **29** (10.0 g, 30.5 mmol) and triisopropyl borate (9.1 mL, 40 mmol) in THF (100 mL) was cooled to −78 °C, and a solution of *n*-butyllithium (25 mL, 40 mmol, 1.6 M in THF) was added dropwise such that the temperature was maintained. Upon completion of addition, the reaction mixture was stirred for an additional 30 min, then quenched with 1 N aqueous HCl (35 mL), and allowed to warm to ambient temperature. The reaction mixture was extracted with EtOAc (100 mL), and the separated organic layer was dried over anhydrous sodium sulfate and concentrated on a rotary evaporator. Hexanes were subsequently added to the crude reaction mixture, which resulted in the formation of a white solid. This slurry was stirred for 1 h at ambient temperature and filtered to afford **31** (8.6 g, 95%). MS (EI): m/z for $C_{14}H_{20}BNO_3$, found 194.0 (MH^+ − Boc).

2-Ethyl-4-(methylsulfonyl)benzoic Acid (33). A stirred solution of 2-bromo-4-(methylsulfonyl)benzoic acid (5.18 g, 18.6 mmol) in THF (40 mL) and MeOH (20 mL) was cooled to 0 °C, and a solution of (trimethylsilyl)diazomethane (12 mL, 24 mmol, 2.0 M in hexanes) was added dropwise such that the temperature was maintained. After being stirred for 2 h, the reaction mixture was concentrated on a rotary evaporator to afford **32** (5.58 g, quantitative) as a colorless solid. ^{1}H NMR (400 MHz, $CDCl_3$): δ 8.24−8.23 (m, 1H), 7.94−7.92 (m, 2H), 3.99 (s, 3H), 3.09 (s, 3H).

A mixture of **32** (200 mg, 0.683 mmol), ethylboronic acid (55 mg, 0.75 mmol), potassium carbonate (283 mg, 2.05 mmol), Ag_2O (395 mg, 1.70 mmol), and [1,1′-bis(diphenylphosphino)ferrocene]-dichloropalladium(II) complex with dichloromethane (50 mg, 0.068 mmol) in THF (5 mL) was stirred in a sealed tube at 80 °C for 18 h. The reaction mixture was filtered through Celite, and the filtrate was concentrated on a rotary evaporator. The residue was purified by flash chromatography (hexanes/ethyl acetate (4:1)) to give methyl 2-ethyl-4-(methylsulfonyl)benzoate (100 mg, 60%) as a colorless oil. ^{1}H NMR (400 MHz, $CDCl_3$): δ 7.99 (d, J = 8.4 Hz, 1H), 7.87 (d, J = 2.0 Hz, 1H), 7.81 (dd, J = 8.0, 2.0 Hz, 1H), 3.95 (s, 3H), 3.08 (s, 3H), 3.04 (q, J = 7.6 Hz, 2H), 1.28 (t, J = 7.6 Hz, 3H).

To a stirred solution of methyl 2-ethyl-4-(methylsulfonyl)benzoate (94 mg, 0.39 mmol) in MeOH (1 mL) and CH_2Cl_2 (1 mL) was added 1 N aqueous NaOH (1 mL), and the resulting mixture was stirred at 45 °C for 2 h. The reaction mixture was cooled to ambient temperature and concentrated on a rotary evaporator. The aqueous residue was acidified with 1 N aqueous HCl to pH 1−2 and extracted with EtOAc (10 mL × 2). The combined organic layers were dried over anhydrous sodium sulfate and concentrated to afford **33** (83 mg, 94%) as a colorless solid. MS (EI): m/z for $C_{10}H_{12}O_4S$, found 227.0 (MH^-).

Compound **34** was prepared from **32** according to a procedure similar to that described for the synthesis of **33**.

Methyl 4-(Methylsulfonyl)-2-propylbenzoate. Colorless oil. ^{1}H NMR (400 MHz, $CDCl_3$): δ 7.99 (d, J = 8.0 Hz, 1H), 7.84 (d, J = 1.6 Hz, 1H), 7.81 (dd, J = 8.0, 2.0 Hz, 1H), 3.95 (s, 3H), 3.07 (s, 3H), 2.98 (t, J = 8.0 Hz, 2H), 1.69−1.63 (m, 2H), 0.99 (t, J = 7.6 Hz, 3H).

4-(Methylsulfonyl)-2-propylbenzoic Acid (34). MS (EI): m/z for $C_{11}H_{14}O_4S$, found 241.0 (MH^-).

2-(Ethylamino)-4-(methylsulfonyl)benzoic Acid (35). A solution of **32** (200 mg, 0.683 mmol), ethylamine (200 μL, excess), xantphos (18 mg, 0.03 mmol), Pd_2dba_3 (14 mg, 0.015 mmol), and Cs_2CO_3 (326 mg, 1.00 mmol) in 1,4-dioxane (3 mL) was stirred in a sealed tube at 95 °C for 15 h. The reaction mixture was cooled to ambient temperature and filtered through Celite, and the filtrate was concentrated on a rotary evaporator. The residue was purified by flash chromatography (hexanes/ethyl acetate (4:1)) to afford methyl 2-(ethylamino)-4-(methylsulfonyl)benzoate (39 mg, 22%) as a yellow solid. ^{1}H NMR (400 MHz, $CDCl_3$): δ 8.06 (d, J = 8.4 Hz, 1H), 7.88 (br s, 1H), 7.20 (d, J = 2.0 Hz, 1H), 7.04 (dd, J = 8.4, 2.0 Hz, 1H), 3.90 (s, 3H), 3.33−3.26 (m, 2H), 3.06 (s, 3H), 1.35 (t, J = 7.2 Hz, 3H).

To a stirred solution of methyl 2-(ethylamino)-4-(methylsulfonyl)-benzoate (39 mg, 0.15 mmol) in MeOH (1 mL) and CH_2Cl_2 (1 mL) was added 1 N aqueous NaOH (1 mL), and the resulting mixture was stirred at 45 °C for 1 h. The reaction mixture was cooled to ambient temperature and concentrated on a rotary evaporator. The aqueous residue was acidified to pH 4 with HCl and extracted with EtOAc (10 mL × 2). The combined organic layers were dried over anhydrous sodium sulfate and concentrated to afford **35** (37 mg, quantitative) as a yellow solid. MS (EI): m/z for $C_{10}H_{13}NO_4S$, found 242.0 (MH^-).

3-Fluoro-2-methyl-4-(methylsulfonyl)benzoic Acid (37). To a stirred mixture of 2,3-difluorotoluene (1.9 g, 15 mmol) and Fe (82.7 mg, 1.48 mmol) in chloroform (10 mL) was added bromine (760 μL, 14.8 mmol) slowly at ambient temperature, and the mixture was stirred overnight. Water (10 mL) was added, and the reaction mixture was extracted with Et_2O (20 mL). The separated organic layer was washed with aqueous sodium thiosulfate and brine, dried over anhydrous sodium sulfate, and concentrated on a rotary evaporator. The residue was purified by Kugelrohr distillation to give 1-bromo-3,4-difluoro-2-methylbenzene (2.49 g, 81%) as a colorless oil.

A stirred solution of 1-bromo-3,4-difluoro-2-methylbenzene (2.49 g, 12.0 mmol) in THF (5 mL) was cooled to 0 °C, and a solution of isopropylmagnesium bromide (9.0 mL, 18 mmol, 2 M in THF) was added slowly so that the temperature was maintained. Upon completion of the addition, the resulting stirred mixture was allowed to warm to ambient temperature for 24 h. Carbon dioxide, generated from dry ice, was introduced to the reaction mixture for 10 min, and the resulting mixture was stirred for an additional 30 min. The reaction mixture was quenched with H_2O (20 mL), and the volatile solvents were removed on a rotary evaporator. The resulting aqueous layer was acidified with concentrated HCl to pH 1−2. The white precipitate that formed was filtered, washed with water and cold hexanes, and dried in vacuo to afford **36** (1.67 g, 81%). ^{1}H NMR (400 MHz, DMSO-d_6): δ 13.10 (br s, 1H), 7.72−7.68 (m, 1H), 7.33 (dd, J = 18.4, 8.8 Hz, 1H), 2.48 (s, 3H). MS (EI): m/z for $C_8H_6F_2O_2$, found 171.0 (MH^-).

To a stirred solution of **36** (700 mg, 4.1 mmol) in DMSO (5 mL) was added NaOH (164 mg, 4.1 mmol), and the mixture was stirred at ambient temperature for 30 min. To this mixture was added sodium thiomethoxide (342 mg, 4.9 mmol), and the resulting mixture was warmed to 55−60 °C for 4 h. The reaction mixture was cooled to 0 °C and quenched with H_2O (10 mL). The resulting mixture was acidified with concentrated HCl to pH 1−2. The white precipitate was collected by filtration, washed with water, and dried in vacuo to afford 3-fluoro-2-methyl-4-(thiomethyl)benzoic acid (879 mg, quantitative), which was used in the next step without further purification. MS (EI): m/z for $C_9H_9FO_2S$, found 199.0 (MH^-).

To a stirred suspension of 3-fluoro-2-methyl-4-(thiomethyl)benzoic acid (879 mg, 4.1 mmol) in acetone (10 mL) and H_2O (10 mL) were added NaOH (330 mg, 8.3 mmol) and sodium bicarbonate (680 mg, 8.1 mmol). The stirred mixture was cooled to 0 °C, and Oxone (4 g) was added portionwise over 10 min. The reaction was monitored by LC/MS. Upon the completion of the reaction, concentrated HCl was added to acidify the mixture to pH 2−3. The white precipitate that formed was collected by filtration, washed with water, and dried. The precipitate was resuspended in water (10 mL), stirred vigorously at ambient temperature for 1 h, filtered, washed with water and hexanes, and dried in vacuo to afford **37** (886 mg, 94%) as a white powder. ^{1}H NMR (400 MHz, DMSO-d_6): δ 13.74 (br s, 1H), 7.82−7.76 (m, 2H), 3.37 (s, 3H), 2.47 (s, 3H). MS (EI): m/z for $C_9H_9FO_4S$, found 231.0 (MH^-).

dx.doi.org/10.1021/jm3007933 | J. Med. Chem. XXXX, XXX, XXX−XXX

2-Ethyl-3-fluoro-4-(methylsulfonyl)benzoic Acid (39). To a stirred solution of 2,3-difluorophenylacetic acid (17.2 g, 100 mmol) in THF (150 mL) was added borane−dimethyl sulfide complex solution (75 mL, 150 mmol, 2 M in THF) over the course of 1 h using a dropping funnel. The reaction mixture started to reflux spontaneously. After being stirred for an additional 3 h, it was cooled to 0 °C, and excess MeOH (20 mL) was added carefully to the reaction mixture. The stirred mixture was allowed to warm to ambient temperature for 1 h and then concentrated on a rotary evaporator. The residue was diluted with dichloromethane (100 mL), washed with aqueous sodium bicarbonate (100 mL), dried over anhydrous sodium sulfate, and concentrated on a rotary evaporator to give 2-(2,3-difluorophenyl)-ethanol (15.6 g, 99%), which was used in the next step without further purification. GC/MS: m/z for $C_8H_8F_2O$, found 158 (M^+).

To a stirred solution of 2-(2,3-difluorophenyl)ethanol (15.6 g, 98.6 mmol) and Et_3N (20.6 mL, 148 mmol) in dichloromethane (100 mL) was added TsCl (20.7 g, 109 mmol). The reaction mixture was stirred for 5 h at ambient temperature and then diluted with dichloromethane (200 mL). The resulting solution was washed with water (100 mL) and brine (100 mL), dried over anhydrous sodium sulfate, and concentrated on a rotary evaporator to afford (2,3-difluorophenyl)-ethyl 4-methylbenzenesulfonate (29.6 g, 96%), which was used in the next step without further purification.

To a stirred mixture of (2,3-difluorophenyl)ethyl 4-methylbenzene-sulfonate (29.6 g, 94.8 mmol) in acetone (150 mL) was added LiBr (42.8 g, 492 mmol), and the reaction was heated to reflux for 3 h. The mixture was cooled to ambient temperature and concentrated on a rotary evaporator. The residue was partitioned with water (200 mL) and hexanes (200 mL). The separated aqueous layer was extracted with hexanes (100 mL). The combined organic layers were then washed with brine, dried over anhydrous sodium sulfate, concentrated on a rotary evaporator, and purified by flash chromatography (hexanes) to give 1-(2-bromoethyl)-2,3-difluorobenzene (19.4 g, 89%). GC/MS: m/z for $C_8H_7BrF_2$, found 142 (M − Br).

To a stirred suspension of Mg (4.26 g, 175 mmol) in Et_2O (50 mL) was added 1,2-dibromoethane (0.755 mL, 8.76 mmol), and the mixture was allowed to stir for 10 min at ambient temperature. The flask was affixed with a reflux condenser, and a solution of 1-(2-bromoethyl)-2,3-difluorobenzene (19.4 g, 87.6 mmol) and 1,2-dibromoethane (0.755 mL, 8.76 mmol) in Et_2O (50 mL) was added over 30 min such that the ether warmed to a steady reflux. The stirred reaction was maintained at reflux for 1 h and then allowed to cool to ambient temperature before being further cooled to 0 °C. Aqueous ammonium chloride (50 mL) was carefully added over the course of 1 h to quench the reaction. The resulting mixture was diluted with H_2O (100 mL), and the separated aqueous layer was extracted with Et_2O (100 mL). The combined organic layers were washed with brine, dried over anhydrous sodium sulfate, and filtered. Careful distillation of the filtrate gave **38** (9.5 g, 76%) as a colorless oil. ^{1}H NMR (400 MHz, $CDCl_3$): δ 7.01−6.97 (m, 3H), 2.70 (q, J = 7.6 Hz, 2H), 1.23 (t, J = 7.6 Hz, 3H). GC/MS: m/z for $C_8H_8F_2$, found 142 (M^+).

Compound **39** was prepared from compound **38** according to a procedure similar to that described for the synthesis of compound **37**. ^{1}H NMR (400 MHz, DMSO-d_6): δ 13.73 (br s, 1H), 7.82−7.76 (m, 2H), 3.76 (s, 3H), 2.94 (q, J = 7.2 Hz, 2H), 1.81 (t, J = 7.2 Hz, 3H). MS (EI): m/z for $C_{10}H_{11}FO_4S$, found 245.0 (MH^-).

2,2,2-Trifluoro-1-(4-(7-(quinolin-3-yl)-2,3,4,5-tetrahydrobenz[*f*][1,4]oxazepin-4-ylcarbonyl)phenyl)-ethanone (1). A mixture of **29** (327 mg, 1.00 mmol), quinolin-3-ylboronic acid (200 mg, 1.15 mmol), potassium carbonate (414 mg, 3.0 mmol), and [1,1′-bis(diphenylphosphino)ferrocene]dichloro-palladium(II) complex with dichloromethane (94 mg, 0.12 mmol) in DME (5 mL) was heated to 80 °C for 2 h. The reaction mixture was cooled to ambient temperature and concentrated on a rotary evaporator, and the residue was purified by flash chromatography (hexanes/ethyl acetate (2:1)) to give **40** (282 mg, 75%) as a white solid. MS (EI): m/z for $C_{23}H_{24}N_2O_3$, found 377.1 (MH^-).

To a stirred solution of **40** (282 mg, 0.75 mmol) in 1,4-dioxane (5 mL) was added a solution of HCl (2 mL, 8 mmol, 4 M in 1,4-dioxane), and the resulting mixture was stirred at ambient temperature overnight. The reaction mixture was concentrated on a rotary evaporator to give 7-(quinolin-3-yl)-2,3,4,5-tetrahydrobenz[*f*][1,4]oxazepine dihydrochloride (259 mg, quantitative), which was used without further purification. 7-(Quinolin-3-yl)-2,3,4,5-tetrahydrobenz[*f*][1,4]oxazepine (**1b**) was obtained from basic workup of a sample with aqueous sodium bicarbonate that was extracted with EtOAc (2×). The combined organic layers were dried over anhydrous sodium sulfate and concentrated on a rotary evaporator, and the residue was purified by reverse-phase HPLC (acetonitrile/aqueous ammonium acetate buffer solution, 20−100% gradient) to give **1b** as a white powder after lyophilization. ^{1}H NMR (400 MHz, CD_3OD): δ 9.38 (d, J = 2.4 Hz, 1H), 9.04 (s, 1H), 8.23 (d, J = 8.0 Hz, 1H), 8.18 (d, J = 8.4 Hz, 1H), 8.00−7.93 (m, 3H), 7.87−7.85 (m, 1H), 7.36 (d, J = 8.8 Hz, 1H), 4.56 (s, 2H), 4.37−4.35 (m, 2H), 3.69−3.66 (m, 2H). MS (EI): m/z for $C_{18}H_{16}N_2O$, found 277.0 (MH^+).

A mixture of crude 7-(quinolin-3-yl)-2,3,4,5-tetrahydrobenz[*f*][1,4]-oxazepine dihydrochloride (229 mg, 0.66 mmol), *N*,*N*-diisopropylethyl-amine (0.575 mL, 3.3 mmol), and 4-(2,2,2-trifluoroacetyl)benzoic acid (173 mg, 0.79 mmol) in DMF (5 mL) was treated with *O*-(7-azabenzotriazol-1-yl)-*N*,*N*,*N*′,*N*′-tetramethyluronium hexafluoro-phosphate (326 mg, 0.86 mmol). After being stirred for 30 min at ambient temperature, the reaction mixture was diluted with saturated sodium bicarbonate (20 mL) and was extracted with EtOAc (30 mLx2). The combined organic layers were dried over anhydrous sodium sulfate and concentrated on a rotary evaporator, and the residue was purified by reverse-phase HPLC (acetonitrile/aqueous ammonium acetate buffer solution, 20−100% gradient) to give **1** (211 mg, 67%) as a white powder after lyophilization. ^{1}H NMR (400 MHz, DMSO-d_6): δ (rotamers are observed) 9.27 and 9.10 (s, 1H), 8.66 and 8.38 (s, 1H), 8.09−7.64 (m, 8H), 7.45 and 7.32 (d, J = 7.2 Hz, 2H), 7.16 and 6.98 (s, 1H), 4.93 and 4.53 (s, 2H), 4.32 and 4.22 (br s, 2H), 4.07 and 3.77 (br s, 2H). MS (EI): m/z for $C_{27}H_{19}F_3N_2O_3$, found 477.0 (MH^+).

Compounds **1c**, **2**−**5**, and **10** were prepared from **29** and the corresponding boronic acid or 4,4,5,5-tetramethyl-1,3,2-dioxaborolane according to a procedure similar to that described for the synthesis of compound **1**. Compound **1a** was prepared from 2,3,4,5-tetrahydro-1,4-benzoxazepine and 4-(2,2,2-trifluoroacetyl)benzoic acid.

2,2,2-Trifluoro-1-(4-(2,3,4,5-tetrahydrobenz[*f*][1,4]oxazepin-4-ylcarbonyl)phenyl)ethanone (1a). ^{1}H NMR (400 MHz, DMSO-d_6): δ (rotamers are observed) 8.13 and 8.10 (d, J = 8.0 Hz, 2H), 7.51−7.45 (m, 2H), 7.28−7.04 (m, 3H), 7.00−6.97 and 6.61−6.59 (m, 1H), 4.83 and 4.41 (s, 2H), 4.25 and 4.16 (t, J = 8.4 Hz, 2H), 4.04 and 3.75 (t, J = 8.4 Hz, 2H). MS (EI): m/z for $C_{18}H_{14}F_3NO_3$, found 350.0 (MH^+).

Phenyl(7-(quinolin-3-yl)-2,3-dihydrobenz[*f*][1,4]oxazepin-4(5*H*)-yl)methanone (1c). ^{1}H NMR (400 MHz, $CDCl_3$): δ (rotamers are observed) 9.20 and 9.03 (s, 1H), 8.35 and 8.16 (s, 1H), 8.14 (d, J = 8.8 Hz, 1H), 7.91−8.31 (m, 1H), 7.76−7.58 (m, 3H), 7.52−7.37 (m, 5H), 7.23−7.19 (m, 1H), 6.93 (s, 1H), 4.93 and 4.55 (s, 2H), 4.31 and 4.19 (br s, 2H), 4.10−3.87 (br s, 2H). MS (EI): m/z for $C_{25}H_{20}N_2O_2$, found 381.0 (MH^+).

2,2,2-Trifluoro-1-(4-(7-(naphthalen-2-yl)-2,3,4,5-tetrahydrobenz[*f*][1,4]oxazepin-4-ylcarbonyl)phenyl)-ethanone (2). ^{1}H NMR (400 MHz, $CDCl_3$): δ (rotamers are observed) 8.20 and 8.14 (d, J = 7.6 Hz, 2H), 7.93−7.74 (m, 4H), 7.63 and 7.61 (d, J = 2.4 Hz, 1H), 7.58−7.48 (m, 5H), 7.20 and 7.17 (d, J = 3.6 Hz, 1H), 6.91 (br s, 1H), 4.94 and 4.50 (s, 2H), 4.31 and 4.21 (t, J = 4.0 Hz, 2H), 4.10 and 3.80 (t, J = 4.0 Hz, 2H). MS (EI): m/z for $C_{28}H_{20}F_3NO_3$, found 476.0 (MH^+).

2,2,2-Trifluoro-1-(4-(7-phenyl-2,3,4,5-tetrahydrobenz[*f*]-[1,4]oxazepin-4-ylcarbonyl)phenyl)ethanone (3). ^{1}H NMR (400 MHz, DMSO-d_6): δ (rotamers are observed) 7.72−7.66 (m, 5H), 7.53 and 7.51 (d, J = 2.4 Hz, 1H), 7.46−7.28 (m, 5H), 7.11−7.05 (m, 1H), 4.85 and 4.48 (s, 2H), 4.26 amd 4.16 (br s, 2H), 4.02 and 3.74 (br s, 2H). MS (EI): m/z for $C_{24}H_{18}F_3NO_3$, found 426.0 (MH^+).

2,2,2-Trifluoro-1-(4-(7-(pyridin-3-yl)-2,3,4,5-tetrahydrobenz-[*f*][1,4]oxazepin-4-ylcarbonyl)phenyl)ethanone (4). ^{1}H NMR (400 MHz, DMSO-d_6): δ (rotamers are observed) 8.95 and 8.87 (s, 1H), 8.70 and 8.52 (br s, 1H), 8.07−8.03 (m, 1H), 7.79−7.26 (m, 6H), 7.11−7.06 (m, 1H), 6.94−6.90 (m, 1H), 4.86 and 4.73 (s, 2H),

dx.doi.org/10.1021/jm3007933 | J. Med. Chem. XXXX, XXX, XXX−XXX

4.26 and 4.18 (br s, 2H), 4.00 and 3.72 (br s, 2H). MS (EI): m/z for $C_{23}H_{17}F_3N_2O_3$, found 427.0 (MH^+).

N-(3-(4-(4-(2,2,2-Trifluoroacetyl)benzoyl)-2,3,4,5-tetrahydrobenz[*f*][1,4]oxazepin-7-yl)phenyl)acetamide (5). ^{1}H NMR (400 MHz, DMSO-d_6): δ (rotamers are observed) 10.06 and 10.02 (s, 1H), 7.85 and 7.83 (s, 1H), 7.73−7.64 (m, 3H), 7.60 and 7.58 (s, 1H), 7.47−7.06 (m, 5H), 7.30 and 6.71 (br s, 1H), 4.84 and 4.48 (s, 2H), 4.27 and 4.16 (br s, 2H), 4.02 and 3.74 (br s, 2H), 2.07 (s, 3H). MS (EI): m/z for $C_{26}H_{21}F_3N_2O_4$, found 483.0 (MH^+).

1-(4-(7-(1*H*-Pyrazol-4-yl)-2,3,4,5-tetrahydrobenz[*f*][1,4]-oxazepin-4-ylcarbonyl)phenyl)-2,2,2-trifluoroethanone (10). ^{1}H NMR (400 MHz, DMSO-d_6): δ (rotamers are observed) 12.92 (s, 1H), 8.18−7.58 (m, 5H), 7.46−7.41 (m, 2H), 7.29−6.95 (m, 2H), 4.80 and 4.40 (s, 2H), 4.19 and 4.11 (br s, 2H), 4.00 and 3.71 (br s, 2H). MS (EI): m/z for $C_{21}H_{16}F_3N_3O_3$, found 416.0 (MH^+).

1-(4-(7-(1*H*-Indazol-6-yl)-2,3,4,5-tetrahydrobenz[*f*][1,4]-oxazepin-4-ylcarbonyl)phenyl)-2,2,2-trifluoroethanone (6). A stirred mixture of **31** (293 mg, 1.0 mmol), 6-bromo-1*H*-indazole (197 mg, 1.0 mmol), triethylamine (348 μL, 2.5 mmol), and [1,1′-bis(diphenylphosphino)ferrocene]dichloropalladium(II) complex with dichloromethane (82 mg, 0.10 mmol) in DME (5 mL) and H_2O (1 mL) was heated to 90 °C for 4 h. The reaction mixture was cooled to ambient temperature, concentrated on a rotary evaporator, and purified by flash chromatography (hexanes/ethyl acetate (1:1)) to give **41** (288 mg, 79%). MS (EI): m/z for $C_{21}H_{23}N_3O_3$, found 366.0 (MH^+).

To a solution of **41** (288 mg, 0.79 mmol) in 1,4-dioxane (5 mL) was added a solution of HCl (2 mL, 8 mmol, 4 M in 1,4-dioxane) and the resulting mixture was stirred at ambient temperature for overnight. The reaction mixture was concentrated on a rotary evaporator to give 7-(1*H*-indazol-6-yl)-2,3,4,5-tetrahydrobenz[*f*][1,4]oxazepine dihydrochloride (269 mg, quant.) which was used in the next step without further purification.

A mixture of crude 7-(1*H*-indazol-6-yl)-2,3,4,5-tetrahydrobenz[*f*]-[1,4]oxazepine dihydrochloride (269 mg, 0.79 mmol), *N*,*N*-diisopropylethylamine (0.688 mL, 3.9 mmol) and 4-(2,2,2-trifluoroacetyl)-benzoic acid (207 mg, 0.95 mmol) in DMF (5 mL) was treated with *O*-(7-azabenzotriazol-1-yl)-*N*,*N*,*N*′,*N*′-tetramethyluronium hexafluorophosphate (390 mg, 1.03 mmol). After stirring for 30 min at ambient temperature, the reaction mixture was diluted with saturated sodium bicarbonate (20 mL) and the aqueous layer was extracted with EtOAc (30 mL × 2). The combined organic layers were dried over anhydrous sodium sulfate and concentrated on a rotary evaporator, and the residue was purified by reverse phase HPLC (acetonitrile/aqueous ammonium acetate buffer solution; 20−100% gradient) to give **6** (272 mg, 74%) as a white powder after lyophilization. ^{1}H NMR (400 MHz, DMSO-d_6): δ (rotamers are observed) 13.13 (s, 1H), 8.10 (s, 1H), 7.85−7.51 (m, 7H), 7.43−7.32 (m, 2H), 7.18−7.08 (m, 1H), 4.89 and 4.53 (d, J = 11.2 Hz, 2H), 4.28 and 4.17 (br s, 2H), 4.04 and 3.76 (br s, 2H). MS (EI): m/z for $C_{25}H_{18}F_3N_3O_3$, found 466.0 (MH^+).

Compounds **7**, **11**−**28** were prepared according to a similar procedure as described for the synthesis of compound **6**. Compound **8** was prepared from 7-(1*H*-indazol-6-yl)-2,3,4,5-tetrahydrobenz[*f*]-[1,4]oxazepine dihydrochloride and 4-acetylbenzoic acid.

1-(4-(7-(1*H*-Indazol-5-yl)-2,3,4,5-tetrahydrobenz[*f*][1,4]-oxazepin-4-ylcarbonyl)phenyl)-2,2,2-trifluoroethanone (7). ^{1}H NMR (400 MHz, DMSO-d_6): δ (rotamers are observed) 13.12 and 13.08 (s, 1H), 8.08 and 8.07 (s, 2H), 7.83−7.49 (m, 6H), 7.43−7.14 (m, 2H), 7.11−6.91 (m, 1H), 4.88 and 4.52 (d, J = 11.2 Hz, 2H), 4.30−4.27 and 4.16−4.14 (m, 2H), 4.05−4.00 and 3.74−3.70 (m, 2H). MS (EI): m/z for $C_{25}H_{18}F_3N_3O_3$, found 466.0 (MH^+).

1-(4-(7-(1*H*-Indazol-6-yl)-2,3,4,5-tetrahydrobenz[*f*][1,4]-oxazepin-4-ylcarbonyl)phenyl)ethanone (8). ^{1}H NMR (400 MHz, DMSO-d_6): δ (rotamers are observed) 13.14 and 13.11 (s, 1H), 8.09 and 8.08 (s, 1H), 8.06 (d, J = 7.6 Hz, 2H), 7.85−7.38 (m, 6H), 7.22−6.91 (m, 2H), 4.89 and 4.55 (s, 2H), 4.31 and 4.16 (br s, 2H), 4.04 and 3.73 (br s, 2H), 2.61 (s, 3H). MS (EI): m/z for $C_{25}H_{21}N_3O_3$, found 412.0 (MH^+).

1-(4-(7-(1-Methyl-*H*-indazol-6-yl)-2,3,4,5-tetrahydrobenz[*f*]-[1,4]oxazepin-4-ylcarbonyl)phenyl)ethanone (9). To a stirred solution of **8** (41 mg, 0.1 mmol) in DMF (2 mL) was added K_2CO_3 (42 mg, 0.3 mmol) and iodomethane (0.1 mL, 1.6 mmol). The reaction mixture was stirred at ambient temperature for overnight. The crude mixture was directly purified by reverse phase HPLC (acetonitrile/aqueous ammonium acetate buffer solution; 20−100% gradient) to give **9** (24 mg, 54%) as a white powder after lyophilization. ^{1}H NMR (400 MHz, DMSO-d_6): δ (rotamers are observed) 8.06−8.00 (m, 3H), 7.92−7.40 (m, 6H), 7.26−6.97 (m, 2H), 4.91 and 4.55 (s, 2H), 4.31 and 4.17 (br s, 2H), 4.12 and 4.08 (s, 3H), 4.06 and 3.74 (br s, 2H), 2.61 (s, 3H). MS (EI): m/z for $C_{26}H_{23}N_3O_3$, found 426.0 (MH^+).

1-(4-(7-(1*H*-Benz[*d*]imidazol-6-yl)-2,3,4,5-tetrahydrobenz[*f*]-[1,4]oxazepin-4-ylcarbonyl)phenyl)-2,2,2-trifluoroethanone (11). ^{1}H NMR (400 MHz, DMSO-d_6): δ (rotamers are observed) 12.51 and 12.43 (s, 1H), 8.26 and 8.25 (s, 1H), 7.90−7.43 (m, 8H), 7.35−7.30 (m, 1H), 7.10−7.06 and 6.76−6.74 (m, 1H), 4.86 and 4.52 (br s, 2H), 4.26 and 4.16 (br s, 2H), 4.03 and 3.75 (br s, 2H). MS (EI): m/z for $C_{25}H_{18}F_3N_3O_3$: 466.0 (MH^+).

2,2,2-Trifluoro-1-(4-(7-(2-methyl-1*H*-benz[*d*]imidazol-6-yl)-2,3,4,5-tetrahydrobenz[*f*][1,4]oxazepin-4-ylcarbonyl)phenyl)-ethanone (12). ^{1}H NMR (400 MHz, DMSO-d_6): δ (rotamers are observed) 12.30 (br s, 1H), 8.10 and 7.81 (br s, 1H), 7.71−7.65 (m, 4H), 7.57−7.42 (m, 3H), 7.33−6.74 (m, 2H), 4.86 and 4.52 (br s, 2H), 4.25 and 4.15 (br s, 2H), 4.04 and 3.75 (br s, 2H), 2.55 (s, 3H). MS (EI): m/z for $C_{26}H_{20}F_3N_3O_3$, found 480.0 (MH^+).

(7-(1*H*-Benz[*d*]imidazol-6-yl)-2,3-dihydrobenz[*f*][1,4]-oxazepin-4(5*H*)-yl)(4-(trifluoromethyl)phenyl)methanone (13) (HCl Salt). ^{1}H NMR (400 MHz, DMSO-d_6): δ (rotamers are observed) 9.49 and 9.45 (s, 1H), 8.03−7.62 (m, 8H), 7.49−6.96 (m, 2H), 4.91 and 4.58 (s, 2H), 4.33 and 4.19 (br s, 2H), 4.05 and 3.74 (br s, 2H). MS (EI): m/z for $C_{24}H_{18}F_3N_3O_2$, found 438.0 (MH^+).

4-(7-(1*H*-Benz[*d*]imidazol-6-yl)-2,3,4,5-tetrahydrobenz[*f*]-[1,4]oxazepin-4-ylcarbonyl)benzenesulfonamide (14). ^{1}H NMR (400 MHz, DMSO-d_6): δ (rotamers are observed) 12.53 (br s, 1H), 8.26 (s, 1H), 7.91−7.46 (m, 10H), 7.30−6.81 (m, 2H), 4.88 and 4.56 (s, 2H), 4.28 and 4.16 (br s, 2H), 4.04 and 3.73 (br s, 2H). MS (EI): m/z for $C_{23}H_{20}N_4O_4S$, found 449.0 (MH^+).

4-(7-(1*H*-Benz[*d*]imidazol-6-yl)-2,3,4,5-tetrahydrobenz[*f*]-[1,4]oxazepin-4-ylcarbonyl)-*N*-methylbenzenesulfonamide (15). ^{1}H NMR (400 MHz, DMSO-d_6): δ (rotamers are observed) 12.51 and 12.42 (s, 1H), 8.25 (br s, 1H), 7.93−7.47 (m, 9H), 7.31−6.76 (m, 2H), 4.88 and 4.53 (s, 2H), 4.27 and 4.16 (br s, 2H), 4.05 and 3.73 (br s, 2H), 2.45−2.35 (m, 3H). MS (EI): m/z for $C_{24}H_{22}N_4O_4S$, found 463.0 (MH^+).

(7-(1*H*-Benz[*d*]imidazol-6-yl)-2,3-dihydrobenz[*f*][1,4]-oxazepin-4(5*H*)-yl)(4-methylsulfonyl)phenyl)methanone (16). ^{1}H NMR (400 MHz, DMSO-d_6): δ (rotamers are observed) 12.52 and 12.44 (s, 1H), 8.25 and 8.24 (s, 1H), 8.02−7.90 (m, 2H), 7.74−7.49 (m, 6H), 7.29−6.85 (m, 2H), 4.88 and 4.53 (s, 2H), 4.28 and 4.16 (br s, 2H), 4.05 and 3.72 (br s, 2H), 3.27 (br s, 3H). MS (EI): m/z for $C_{24}H_{21}N_3O_4S$, found 448.0 (MH^+).

(7-(1*H*-Benz[*d*]imidazol-6-yl)-2,3-dihydrobenz[*f*][1,4]-oxazepin-4(5*H*)-yl)(4-ethylsulfonyl)phenyl)methanone (17). ^{1}H NMR (400 MHz, $CDCl_3$): δ 8.14−7.56 (m, 4H), 7.55−7.41 (m, 4H), 7.23 (s, 1H), 7.15 (d, J = 8.4 Hz, 1H), 6.33 (d, J = 2.0 Hz, 1H), 4.91 and 4.42 (s, 2H), 4.26−3.78 (m, 4H), 3.28 (q, J = 7.6 Hz, 2H), 2.12 and 2.02 (s, 1H), 1.38 (t, J = 7.6 Hz, 3H). MS (EI): m/z for $C_{25}H_{23}N_3O_4S$, found 462.0 (MH^+).

(7-(1*H*-Benz[*d*]imidazol-6-yl)-2,3-dihydrobenz[*f*][1,4]-oxazepin-4(5*H*)-yl)(2-methyl-4-(methylsulfonyl)phenyl)-methanone (18). ^{1}H NMR (400 MHz, $CDCl_3$): δ 8.11−7.80 (m, 4H), 7.54−7.38 (m, 3H), 7.28−7.14 (m, 2H), 6.29 (s, 1H), 4.39−4.10 (m, 6H), 3.21 (s, 3H), 2.12 (s, 1H), 2.02 (s, 3H). MS (EI): m/z for $C_{25}H_{23}N_3O_4S$, found 462.0 (MH^+).

(7-(1*H*-Benz[*d*]imidazol-6-yl)-2,3-dihydrobenz[*f*][1,4]-oxazepin-4(5*H*)-yl)(2-ethyl-4-(methylsulfonyl)phenyl)-methanone (19). ^{1}H NMR (400 MHz, $CDCl_3$): δ (rotamers are observed) 8.10 (s, 1H), 8.03−7.79 (m, 3H), 7.53 (dd, J = 8.0, 2.0 Hz, 1H), 7.43 (dd, J = 8.8, 1.6 Hz, 1H), 7.33 (d, J = 7.6 Hz, 1H), 7.26 (s, 1H), 7.15 (d, J = 8.4 Hz, 1H), 6.29 (d, J = 2.4 Hz, 1H), 4.38−4.20 (m, 6H), 3.21 (s, 3H), 2.54−2.44 and 2.29−2.20 (m, 2H), 2.12 (br s, 1H),

dx.doi.org/10.1021/jm3007933 | J. Med. Chem. XXXX, XXX, XXX−XXX

1.14 (t, J = 7.6 Hz, 3H). MS (EI): m/z for $C_{26}H_{25}N_3O_4S$, found 476.0 (MH^+).

(7-(1*H*-Benz[*d*]imidazol-6-yl)-2,3-dihydrobenz[*f*][1,4]-oxazepin-4(5*H*)-yl)(4-(methylsulfonyl)-2-propylphenyl)-methanone (20). ^{1}H NMR (400 MHz, $CDCl_3$): δ (rotamers are observed) 8.11 (br s, 1H), 7.99 (s, 1H), 7.97 (d, J = 2.0 Hz, 1H), 7.81 (dd, J = 18.8, 10.0 Hz, 1H), 7.53 (dd, J = 8.4, 2.4 Hz, 1H), 7.42 (dd, J = 8.8, 1.6 Hz, 1H), 7.32 (d, J = 8.0 Hz, 1H), 7.27 (s, 1H), 7.15 (d, J = 8.0 Hz, 1H), 6.29 (d, J = 2.4 Hz, 1H), 4.38 (d, J = 15.6 Hz, 1H), 4.25 (d, J = 14.8 Hz, 1H), 4.23 (br s, 4H), 3.21 (s, 3H), 2.45−2.37 (m 1H), 2.24−2.16 (m, 1H), 2.12 (s, 1H), 1.70−1.61 (m 1H), 1.50−1.43 (m, 1H), 0.89 and 0.86 (t, J = 7.2 Hz, 3H). MS (EI): m/z for $C_{27}H_{27}N_3O_4S$, found 490.0 (MH^+).

(7-(1*H*-Benz[*d*]imidazol-6-yl)-2,3-dihydrobenz[*f*][1,4]-oxazepin-4(5*H*)-yl)(2-(ethylamino)-4-(methylsulfonyl)phenyl)-methanone (21). ^{1}H NMR (400 MHz, $CDCl_3$): δ 8.10 (s, 1H), 7.80 (d, J = 8.0 Hz, 1H), 7.52 (dd, J = 8.4, 2.4 Hz, 1H), 7.44−7.39 (m, 3H), 7.25−7.23 (m, 2H), 7.13 (d, J = 8.4 Hz, 1H), 6.47 (s, 1H), 4.46 (br s, 2H), 4.24−4.18 (m, 5H), 3.19 (s, 3H), 2.94 (br s, 2H), 2.12 (s, 1H), 0.99 (t, J = 6.8 Hz, 3H). MS (EI): m/z for $C_{26}H_{26}N_4O_4S$, found 491.0 (MH^+).

(7-(1*H*-Benz[*d*]imidazol-6-yl)-2,3-dihydrobenz[*f*][1,4]-oxazepin-4(5*H*)-yl)(2-chloro-4-(methylsulfonyl)phenyl)-methanone (22). ^{1}H NMR (400 MHz, $CDCl_3$): δ 8.22 (s, 1H), 8.18 (d, J = 1.6 Hz, 1H), 8.04 (dd, J = 8.0, 2.0 Hz, 1H), 7.81 (d, J = 8.4 Hz, 1H), 7.53 (dd, J = 8.4, 2.4 Hz, 1H), 7.45 (dd, J = 8.4, 1.6 Hz, 1H), 7.36 (d, J = 8.0 Hz, 1H), 7.23 (s, 1H), 7.16 (d, J = 8.4 Hz, 1H), 6.35 (d, J = 2.4 Hz, 1H), 4.45 (d, J = 15.6 Hz, 1H), 4.42−4.32 (m, 2H), 4.25 (d, J = 15.6 Hz, 1H), 4.16−4.05 (m, 2H), 3.24 (s, 3H), 2.11 (s, 1H). MS (EI): m/z for $C_{24}H_{20}ClN_3O_4S$, found 482.0 (MH^+).

(7-(1*H*-Benz[*d*]imidazol-6-yl)-2,3-dihydrobenz[*f*][1,4]-oxazepin-4(5*H*)-yl)(2-bromo-4-(methylsulfonyl)phenyl)-methanone (23). ^{1}H NMR (400 MHz, $CDCl_3$): δ 8.34 (d, J = 1.6 Hz, 1H), 8.10 (d, J = 1.6 Hz, 1H), 8.08 (s, 1H), 7.80 (d, J = 8.0 Hz, 1H), 7.54 (dd, J = 8.4, 2.4 Hz, 1H), 7.42 (dd, J = 8.4, 2.0 Hz, 1H), 7.35 (d, J = 8.0 Hz, 1H), 7.22 (s, 1H), 7.16 (d, J = 8.4 Hz, 1H), 6.35 (s, 1H), 4.44 (d, J = 15.6 Hz, 1H), 4.37−4.32 (m, 2H), 4.26 (d, J = 15.6 Hz, 1H), 4.19−4.08 (m, 2H), 3.23 (s, 3H), 2.12 (s, 1H). MS (EI): m/z for $C_{24}H_{20}BrN_3O_4S$, found 526.0, 528.0 (MH^+).

(7-(1*H*-Benz[*d*]imidazol-6-yl)-2,3-dihydrobenz[*f*][1,4]-oxazepin-4(5*H*)-yl)(3-methyl-4-(methylsulfonyl)phenyl)-methanone (24) (HCl Salt). ^{1}H NMR (400 MHz, DMSO-d_6): δ (rotamers are observed) 9.55 and 9.53 (s, 1H), 8.03−7.78 (m, 4H), 7.64−7.49 (m, 2H), 7.46 and 7.37 (d, J = 8.8 Hz, 1H), 7.31−7.02 (m, 3H), 4.90 and 4.56 (s, 2H), 4.34 and 4.18 (br s, 2H), 4.04 and 3.74 (br s, 2H), 3.25 and 3.17 (s, 3H), 2.65 and 2.46 (s, 3H). MS (EI): m/z for $C_{25}H_{23}N_3O_4S$, found 462.0 (MH^+).

(7-(1*H*-Benz[*d*]imidazol-6-yl)-2,3-dihydrobenz[*f*][1,4]-oxazepin-4(5*H*)-yl)(3-fluoro-2-methyl-4-(methylsulfonyl)-phenyl)methanone (25). ^{1}H NMR (400 MHz, DMSO-d_6): δ (rotamers are observed) 12.49 and 12.00 (br s, 1H), 8.25 (d, J = 8.4 Hz, 1H), 7.83−7.49 (m, 5H), 7.30−6.77 (m, 3H), 4.98−4.85 (m, 1H), 4.53−4.36 (m, 1H), 4.36−3.57 (m, 4H), 3.34 (s, 3H, overlapping with H_2O), 2.13 and 1.78 (d, J = 2.4 Hz, 3H). MS (EI): m/z for $C_{25}H_{22}FN_3O_4S$, found 480.0 (MH^+).

(7-(1*H*-Benz[*d*]imidazol-6-yl)-2,3-dihydrobenz[*f*][1,4]-oxazepin-4(5*H*)-yl)(2-ethyl-3-fluoro-4-(methylsulfonyl)phenyl)-methanone (26). ^{1}H NMR (400 MHz, DMSO-d_6): δ (rotamers are observed) 12.48 and 12.39 (br s, 1H), 8.24 (d, J = 8.0 Hz, 1H), 7.79−7.51 (m, 5H), 7.30−6.79 (m, 3H), 5.03 and 4.83 (d, J = 15.2 Hz, 1H), 4.49 and 4.41 (d, J = 15.6 Hz, 1H), 4.34−3.59 (m, 4H), 3.36 (s, 3H, overlapping with H_2O), 2.69−2.04 (m, 2H), 1.10 and 0.99 (t, J = 7.6 Hz, 3H). MS (EI): m/z for $C_{26}H_{242}FN_3O_4S$, found 494.0 (MH^+).

(7-(6-Aminopyridin-3-yl)-2,3-dihydrobenz[*f*][1,4]oxazepin-4(5*H*)-yl)(4-(methylsulfonyl)phenyl)methanone (27). ^{1}H NMR (400 MHz, DMSO-d_6): δ (rotamers are observed) 8.23 (br s, 1H), 8.04−7.97 (m, 2H), 7.70−7.64 (m, 2H), 7.56 and 6.72 (s, 1H), 7.50−7.40 (m, 2H), 7.05 and 7.01 (d, J = 8.8 Hz, 1H), 6.53 and 6.46 (d, J = 8.8 Hz, 1H), 6.05 (s, 2H), 4.84 and 4.47 (s, 2H), 4.24 and 4.12 (br s, 2H), 4.03 and 3.70 (br s, 2H), 3.28 and 3.26 (s, 3H). MS (EI): m/z for $C_{22}H_{21}N_3O_4S$, found 424.0 (MH^+).

(7-(6-Aminopyridin-3-yl)-2,3-dihydrobenz[*f*][1,4]oxazepin-4(5*H*)-yl)(3-fluoro-2-methyl-4-(methylsulfonyl)phenyl)-methanone (28). ^{1}H NMR (400 MHz, DMSO-d_6): δ (rotamers are observed) 8.24 and 8.03 (d, J = 2.4 Hz, 1H), 7.77 and 7.72 (t, J = 7.6 Hz, 1H), 7.71−7.39 (m, 2H), 7.57 and 6.63 (d, J = 2.4 Hz, 1H), 7.28 and 7.19 (d, J = 7.6 Hz, 1H), 7.04 and 7.02 (d, J = 8.0 Hz, 1H), 6.52 and 6.46 (d, J = 8.8 Hz, 1H), 6.05 (br s, 2H), 4.93−4.31 (m, 2H), 4.28−3.56 (m, 4H), 3.37 and 3.34 (s, 3H), 2.12 and 1.77 (d, J = 1.6 Hz, 3H). ^{13}C NMR (100 MHz, DMSO-d_6): δ 167.3, 167.2, 166.6, 166.6, 158.9, 158.9, 158.4, 158.4, 157.4, 157.2, 155.9, 155.8, 145.4, 145.1, 145.1, 144.0, 143.9, 135.0, 134.7, 132.9, 132.8, 129.4, 129.2, 128.2, 128.2, 128.1, 128.0, 127.0, 126.9, 126.8, 125.9, 125.6, 125.4, 123.6, 123.5, 123.3, 123.1, 122.8, 122.0, 122.0, 121.9, 121.9, 121.2, 120.7, 107.8, 107.8, 70.9, 70.8, 51.1, 51.1, 47.4, 46.5, 43.5, 43.5, 43.5, 43.4, 11.0, 10.9, 10.7, 10.6. IR (KBr pellet): 1623, 1487, 1457, 1423, 1385, 1314, 1269, 1226, 1193, 1144, 1133, 1054, 1031, 962, 821, 768 cm^{-1}. Mp: 204−205 °C. MS (EI): m/z for $C_{23}H_{22}FN_3O_4S$, 456.0 (MH^+). High-resolution MS (FAB MS using glycerol as the matrix): m/z calcd for $C_{23}H_{22}FN_3O_4S$ 456.13878, found 456.13943.

mTOR ELISA Assay. The measurement of mTOR enzyme activity was performed in an ELISA format following the phosphorylation of 4E-BP1 protein. All experiments were performed in the 384-well format. Generally, 0.5 μL of DMSO containing varying concentrations of the test compound was mixed with 15 μL of the enzyme solution. Kinase reactions were initiated with the addition of 15 μL of a solution containing the substrate. The assay conditions were as follows: 0.2 nM mTOR, 10 μM ATP, and 50 nM NHis-tagged 4E-BP1 in 20 mM Hepes, pH 7.2, 1 mM DTT, 50 mM NaCl, 10 mM $MnCl_2$, 0.02 mg/mL BSA, 0.01% CHAPS, 50 mM β-glycerophophate. Following an incubation of 120 min at ambient temperature, 20 μL of the reaction mixture was transferred to a Ni-chelate-coated 384-well plate. The binding step of the 4E-BP1 protein proceeded for 60 min, followed by washing four times each with 50 μL of Tris-buffered saline solution (TBS). Anti-phospho-4E-BP1 rabbit immunoglobulin G (IgG; 20 μL, 1:5000) in 5% BSA−TBST (0.2% Tween-20 in TBS) was added, and the reaction mixuture was further incubated for 60 min. Incubation with a secondary horseradish peroxidase (HRP)-tagged anti-IgG was similarly performed after the primary antibody was washed off (four washes of 50 μL). Following the final wash step with TBST, 20 μL of SuperSignal ELISA Femto (Pierce Biotechnology, 37075) was added and the luminescence measured using an EnVision plate reader. Data are reported as the mean ($n \geq 2$).

PI3Kα Biochemical Assay. PI3Kα activity is measured as the percentage of ATP consumed following the kinase reaction using luciferase−luciferin-coupled chemiluminescence. Reactions were conducted in 384-well white, medium-binding microtiter plates (Greiner). Kinase reactions were initiated by combining test compounds, ATP, substrate (PIP2), and kinase in a 20 μL volume in a buffer solution. The standard PI3Kα assay buffer is composed of 50 mM Tris, pH 7.5, 1 mM EGTA, 10 mM $MgCl_2$, 1 mM DTT, and 0.03% CHAPS. The standard assay concentrations for enzyme, ATP, and substrate are 1.5 nM, 1 μM, and 10 μM, respectively. The reaction mixture was incubated at ambient temperature for approximately 2 h. Following the kinase reaction, a 10 μL aliquot of luciferase−luciferin mix (Promega Kinase-Glo) was added and the chemiluminescence signal measured using a Victor2 plate reader (Perkin-Elmer). Total ATP consumption was limited to 40−60%, and the IC_{50} values of the control compounds correlated well with literature references. Data are reported as the mean ($n \geq 2$).

pS6 (S240/244) ELISA. PC-3 cells (ATCC) were seeded onto 96-well plates (Corning, 3904) in DMEM (Cellgro) containing 10% FBS (Cellgro), 1% NEAA (Cellgro), and 1% penicillin−streptomycin (Cellgro) at 8×10^3 cells per well. The cells were incubated at 37 °C and 5% CO_2 for 48 h, and the growth medium was replaced with serum-free DMEM. Serial dilutions of the test compound in 0.3% DMSO (vehicle) were added to the cells and incubated for 3 h. To fix the cells, medium was removed and 100 μL/well of 4% formaldehyde (Sigma) in TBS was added to each well at ambient temperature for 30 min. The cells were washed three times with 200 μL of TBST and quenched with 100 μL of 0.6% H_2O_2 (VWR International) in TBST

dx.doi.org/10.1021/jm3007933 | J. Med. Chem. XXXX, XXX, XXX−XXX

for 30 min at ambient temperature. The plates were washed three times with 200 μL of TBST and blocked with 100 μL of 5% BSA (Jackson ImmunoResearch) in TBST for 1 h at ambient temperature. Anti-pS6 (S240/244) antibody (Cell Signaling Technology, 2215) or anti-total-S6 antibody (Cell Signaling Technology, 2217) was diluted 1:500 in 5% BSA in TBST. A 50 μL volume of either primary antibody solution was added to the plate to detect pS6 or total S6. After incubation overnight at 4 °C, the plates were washed four times with 200 μL of TBST. Goat antirabbit secondary antibody (Jackson ImmunoResearch) was diluted at 1:15000 in 5% BSA in TBST. A 100 μL volume of antibody solution was added to each well and incubated for 1 h at ambient temperature. The plates were washed three times with 200 μL of TBST and two times with 200 μL of TBS. Chemiluminescent substrate (SuperSignal Elisa Femto) was prepared at rt. A 100 μL volume of chemiluminescent substrate per well was added, and then the plate was shaken for 1 min. Luminescence was read immediately on a Wallac plate reader at a wavelength of 560 nm. After normalization of the pS6 signal to a total S6 signal, IC_{50} values were determined relative to the DMSO-treated control. Data are reported as the mean ($n \geq 2$).

pAKT (S473) ELISA. PC-3 cells (ATCC) were seeded onto 96-well plates (Corning, 3904) in DMEM (Cellgro, 10-013-CV) containing 10% FBS (Cellgro, 35-016-CV), 1% NEAA (Cellgro, 25-025-CI), and 1% penicillin–streptomycin (Cellgro, 30-002-CI) at 8×10^3 cells per well. The cells were incubated at 37 °C and 5% CO_2 for 48 h, and the growth medium was replaced with serum-free DMEM. Serial dilutions of the test compound in 0.3% DMSO (vehicle) were added to the cells and incubated for 2 h and 50 min. The cells were then stimulated for 10 min with 20 ng/mL EGF (US Biologicals, E3374-07A)) for PC-3 or with 1.2 μg/mL Long R^3 IGF-1 (Sigma, I1271) for MCF-7. To fix the cells, medium was removed and 100 μL/well of 4% formaldehyde (Sigma, F8775) in TBS (20 mM Tris, 500 mM NaCl) was added to each well at ambient temperature for 30 min. The cells were washed three times with 200 μL of TBS containing 0.1% Tween 20 (Bio-Rad, 170-6351) (TBST) and quenched with 100 μL of 0.6% H_2O_2 (VWR International, VW3742-1) in TBST for 30 min at rt. The plates were washed three times with 200 μL of TBST and blocked with 100 μL of 5% BSA (Jackson ImmunoResearch, 001-000-173) in TBST for 1 h at rt. Anti-pAKT (S473) antibody (Cell Signaling Technology, 4058) or anti-total-AKT antibody (Cell Signaling Technology, 9272) was diluted 1:400 or 1:500, respectively, in 5% BSA in TBST. A 50 μL volume of either primary antibody solution was added to the plate to detect pAKT (S473) or total AKT. After incubation overnight at 4 °C, the plates were washed four times with 200 μL of TBST. Goat antirabbit secondary antibody (Jackson ImmunoResearch, 111-035-003) was diluted at 1:15000 in 5% BSA in TBST. A 100 μL volume of antibody solution was added to each well and incubated for 1 h at ambient temperature. The plates were washed three times with 200 μL of TBST and two times with 200 μL of TBS. Chemiluminescent substrate (SuperSignal Elisa Femto) was prepared at rt. A 100 μL volume of chemiluminescent substrate per well was added, and then the plate was shaken for 1 min. Luminescence was read immediately on a Wallac plate reader at a wavelength of 560 nm. After normalization of the pAKT signal to a total AKT signal, IC_{50} values were determined relative to the DMSO-treated control. Data are reported as the mean ($n \geq 2$).

In Vivo Pharmacokinetic Studies. Pharmacokinetic studies of **28** were determined in female athymic nude mice, female CD rats, male beagle dogs, and male cynomolgus monkeys. Compound **28** was administered intravenously and by oral gavage at 10 mg/kg as a solution formulated in EPW (5% ethanol/45% PEG400/water + 1:2 HCl (m/m)) to mice, 3 mg/kg as a solution formulated in EPW (5% ethanol/45% PEG400/water + 1:2 HCl (m/m)) to CD rats and male beagle dogs, and 3 mg/kg as a solution formulated in EPW (5% ethanol/45% PEG400/water + 1:1.5 HCl (m/m)) to male cynomolgus monkeys. The plasma levels of **28** were monitored over a 24 h period.

In Vivo Pharmacodynamic Studies. *PC-3 Prostate Adenocarcinoma Model.* PC-3 human prostate adenocarcinoma cells were cultured in vitro in DMEM (Mediatech) supplemented with 20% fetal bovine serum (Hyclone), penicillin–streptomycin, and nonessential amino acids at 37 °C in a humidified 5% CO_2 atmosphere. On day 0, cells were harvested by trypsinization, and 3×10^6 cells (passages 10–14, >95% viability) in 0.1 mL of ice-cold Hank's balanced salt solution were implanted subcutaneously into the hindflank of 5–8 week old male nude mice. When the tumors reached 200–500 mg in size, the mice were administered a single dose of **28**. Scheduled takedown was at 4 h after a single dose. PC-3 tumor lysate was pooled for each group. Phosphor-AKT (S473), phosphor-AKT (T308), phosphor-p70S6K (T389), phosphor-S6 (S240/244), and phosphor-4E-BP1 (T37/46) levels were analyzed by Western immunoblotting and normalized to α-tubulin. α-Tubulin levels were analyzed by Western immunoblotting from the same membrane as the p-S6 and p-4E-BP1 blots.

MCF-7 Breast Adenocarcinama Model. MCF-7 human mammary adenocarcinoma cells were cultured in vitro in DMEM (Cellgro) supplemented with 10% fetal bovine serum (Cellgro), penicillin–streptomycin, and nonessential amino acids at 37 °C in a humidified 5% CO_2 atmosphere. On day 0, cells were harvested by trypsinization, and 5×10^6 cells in 0.1 mL of a solution made of 50% cold Hank's balanced salt solution with 50% growth factor reduced matrigel (Becton Dickinson) were implanted subcutaneously into the hindflank of 5–8 week old female nude mice. When the tumors reached 40–150 mg in size, the mice were administered a single dose of **28**. Scheduled takedown was at 4 h after a single dose. MCF-7 tumor lysate was pooled for each group. Phosphor-AKT (S473), phosphor-AKT (T308), phosphor-p70S6K (T389), phosphor-S6 (S240/244), and phosphor-4E-BP1 (T37/46) levels were analyzed by Western immunoblotting and normalized to α-tubulin. α-Tubulin levels were analyzed by Western immunoblotting from the same membrane as the p-S6 and p-4E-BP1 blots.

Antitumor (MCF-7 Model) Efficacy Studies. Female athymic nude mice (NCr) 5–8 weeks of age and weighing approximately 20–25 g were used. Prior to initiation of study, the animals were allowed to acclimate for a minimum of 48 h. During these studies, the animals were provided food and water ad libitum and housed in a room conditioned at 70–75 °F and 60% relative humidity. A 12 h light and 12 h dark cycle was maintained with automatic timers. MCF-7 tumors were established subcutaneously and staged when the average tumor mass reached 100–200 mg. Compound **28** was orally administered as a solution/fine suspension in water (with a 1:1 molar ratio of 1 N HCl) qd at 50 and 100 mg/kg for 14 days. Tumor mass was determined by measuring perpendicular diameters with a caliper, using the following formula: tumor mass (mg) = [tumor volume = length (mm) × $width^2$ (mm^2)]/2. During the period of study, tumor masses were determined twice weekly and body masses were recorded daily. All animals were examined daily for compound-induced or tumor-related deaths.

AUTHOR INFORMATION

Corresponding Author

*Phone: 82-2-470-9602 (B.G.K.); (813) 974-4642 (J.W.L.). E-mail: byunggyu72kim@gmail.com (B.G.K.); jwleahy@usf.edu (J.W.L.).

Present Addresses

†Asan Institute of Life Science, Songpa-gu, Seoul 138-736, South Korea.

‡Departments of Chemistry and Molecular Medicine and Florida Center of Excellence for Drug Discovery & Innovation, University of South Florida, 3720 Spectrum Blvd., Suite 305, Tampa, FL 33612.

Notes

The authors declare no competing financial interest.

ACKNOWLEDGMENTS

We thank Siamak Dailami for analytical support, Annapurna Sapre and Eric Brooks for conducting the biochemical assay, Jing Ping Yang, Peter Kim, Qiang Wu, Torsten Trowe, Suzanne Crawley, Keith Calkins, Eun Ok Kim, Suresh Selvaraj, and Loan

Hoang for executing cell-based assays, Lory Tan, John Bui, Kendra Kim, Arturo Picones, Jing Wang, Shineal Patel, and Xiang Wu for collecting the reported ADME data, and Atulkumar Ramaiya, Scott Womble, Michael F. Yakes, Joshua Tanguay, and Scott Lam for obtaining PK and conducting PD/efficacy studies.

■ ABBREVIATIONS USED

mTOR, mammalian target of rapamycin; PI3K, phosphoinositide 3-kinase; Akt, v-akt murine thymoma viral oncogene homologue 1; DNA-PK, DNA-activated protein kinase; ATM, ataxia telangiectasia mutated kinase; 4E-BP1, eukaryotic translationa initiation factor 4E binding protein; MLM, mouse liver microsom; PK, pharmacokinetics

■ REFERENCES

(1) Bjornsti, M. A.; Houghton, P. J. The TOR Pathway: A Target for Cancer Therapy. *Nat. Rev. Cancer* **2004**, *4*, 335−348.
(2) Guertin, D. A.; Sabatini, D. M. Defining the Role of mTOR in Cancer. *Cancer Cell* **2007**, *12*, 9−22.
(3) Houghton, P. J.; Huang, S. mTOR as a Target for Cancer Therapy. *Curr. Top. Microbiol. Immunol.* **2004**, *279*, 339−359.
(4) Inoki, K.; Corradetti, M. N.; Guan, K. L. Dysregulation of the TSC-mTOR Pathway in Human Disease. *Nat. Genet.* **2005**, *37*, 19−24.
(5) Jiang, Y. −P.; Ballou, L. M.; Lin, R. Z. Rapamycin-Insensitive Regulation of 4E-BP1 in Regenerating Rat Liver. *J. Biol. Chem.* **2001**, *276*, 10943−10951.
(6) Boylan, J. M.; Anand, P.; Gruppuso, P. A. Ribosomal Protein S6 Phosphorylation and Function during Late Gestation Liver Development in the Rat. *J. Biol. Chem.* **2001**, *276*, 44457−44463.
(7) Thoreen, C. C.; Kang, S. A.; Chang, J. W.; Liu, Q.; Zhang, J.; Gao, Y.; Reichling, L. J.; Sim, T.; Sabatini, D. M.; Gray, N. S. An ATP Competitive Mammalian Target of Rapamycin Inhibitor Reveals Rapamycin-Resistant Functions of mTORC1. *J. Biol. Chem.* **2009**, *284*, 8023−8032.
(8) Feldman, M. E.; Apsel, B.; Uotila, A.; Loewith, R.; Knight, Z. A.; Ruggero, D.; Shokat, K. M. Active-Site Inhibitors of mTOR Target Rapamycin-Resistant Outpurs of mTORC1 and mTORC2. *PLoS Biol.* **2009**, *7*, 371−383.
(9) Finger, D. C.; Salama, S.; Tsou, C.; Harlow, E.; Blenis, J. Mammalian Cell Size Is Controlled by mTOR and Its Downstream Targets S6K1 and 4EBP1/eIF4E. *Gene Dev.* **2002**, *16*, 1472−1487.
(10) Finger, D. C.; Richardson, C. J.; Tee, A. R.; Cheatham, L.; Tsou, C.; Blenis, J. mTOR Controls Cell Cycle Progression through Its Cell Growth Effectors S6K1 and 4E-BP1/Eurkaryotic Translation Initiation Factor 4E. *Mol. Cell. Biol.* **2004**, *24*, 200−216.
(11) Sarbassov, D. D.; Ali, S. M.; Sengupta, S.; Sheen, J. H.; Hsu, P. P.; Bagley, A. F.; Markhard, A. L.; Sabatini, D. M. Prolonged Rapamycin Treatment Inhibits mTORC2 Assembly and Akt/PKB. *Mol. Cell* **2006**, *22*, 159−168.
(12) Choo, A. Y.; Yoon, S. O.; Kim, S. G.; Roux, P. P.; Blenis, J. Rapamycin Differentially Inhibits S6Ks and 4E-BP1 To Mediate Cell-Type-Specific Repression of mRNA Translation. *Proc. Natl. Acad. Sci. U.S.A.* **2008**, *105*, 17414−17419.
(13) Guertin, D. A.; Sabatini, D. M. The Pharmacology of mTOR Inhibition. *Sci. Signaling* **2009**, *2*, 1−6.
(14) Abraham, R. T. PI 3-Kinase Related Kinases: "Big" Players in Stress-Induced Signaling Pathways. *DNA Repair* **2004**, *3*, 883−887.
(15) Park, S.; Chapuis, N.; Bardet, V.; Tamburini, J.; Gallay, N.; Willems, L.; Knight, Z. A.; Shokat, K. M.; Azar, N.; Viguie, F.; Ifrah, N.; Dreyfus, F.; Mayeux, P.; Lacombe, C.; Bouscary, D. PI-103, a Dual Inhibitor of Class IA Phosphatidylinositide 3-Kinase and mTOR, Has Antileukemic Activity in AML. *Leukemia* **2008**, *22*, 1698−1706.
(16) Serra, V.; Markman, B.; Scaltriti, M.; Eichhorn, P. J. A.; Valero, V.; Guzman, M.; Botero, M. L.; Llonch, E.; Atzori, F.; Cosimo, S. D.; Maira, M.; Carcia-Echeverria, C.; Parra, J. L.; Arribas, J.; Baselga, J. NVP-BEZ235, a Dual PI3K/mTOR Inhibitor, Prevents PI3K Signaling and Inhibits the Growth of Cancer Cells with Activating PI3K Mutations. *Cancer Res.* **2008**, *68*, 8022−8030.
(17) Sutherlin, D. P.; Bao, L.; Berry, M.; Castanedo, G.; Chuckowree, I.; Doston, J.; Folkes, A.; Freidman, L.; Goldsmith, R.; Heffron, T.; Lesnick, J.; Lewis, C.; Mathieu, S.; Murray, J.; Nonomiya, J.; Pang, J.; Pegg, N.; Prior, W. W.; Rouge, L.; Salphati, L.; Sampath, D.; Tian, Q.; Tsui, V.; Wan, N. C.; Wang, S.; Wei, B.; Wiesmann, C.; Wu, P.; Zhu, B.; Olivero, A. Discovery of a Potent, Selective, and Orally Available Class I Phosphatidylinositol 3-Kinase (PI3K)/Mammalian Target of Rapamycin (mTOR) Kinase Inhibitor (GDC-0980) for the Treatment of Cancer. *J. Med. Chem.* **2011**, *54*, 7579−7587.
(18) Knight, S. D.; Adams, N. D.; Burgess, J. L.; Chaudhari, A. M.; Darcy, M. G.; Donatelli, C. A.; Luengo, J. I.; Newlander, K. A.; Parrish, C. A.; Ridgers, L.; Sarpong, M. A.; Schmidt, S. J.; Van Aller, G. S.; Carson, J. D.; Diamond, M. A.; Elkins, P. A.; Gardiner, C. M.; Carver, E.; Gilbert, S. A.; Gontarek, R. R.; Jackson, J. R.; Kershner, K. L.; Luo, L.; Raga, K.; Sherk, C. S.; Sung, C.; Sutton, D.; Tummino, P. J.; Wegrzyn, R. J.; Auger, K. R.; Dhanak, D. Discovery of GSK2126458, a Highly Potent Inhibitor of PI3K and the Mammalian Target of Rapamycin. *ACS Med. Chem. Lett.* **2010**, *1*, 39−43.
(19) Garcia-Martinez, J. M.; Moran, J.; Clarke, R. G.; Gray, A.; Cosulich, S. C.; Chresta, C. M.; Alessi, D. R. Ku-0063794 Is a Specific Inhibitor of the Mammalian Target of Rapamycin (mTOR). *Biochem. J.* **2009**, *412*, 29−42.
(20) Yu, K.; Toral-Barza, L.; Shi, C.; Zhang, W.; Lucas, J.; Shor, B.; Kim, J.; Verheijen, J.; Curran, K.; Malwitz, D. J.; Cole, D. C.; Ellingboe, J.; Ayral-Kaloustian, S.; Mansour, T. S.; Gibbons, J. J.; Abraham, R. T.; Nowak, P.; Zask, A. Biochemical, Cellular, and in Vivo Activity of Novel ATP-Competitive and Selective Inhibitors of the Mammalian Target of Rapamycin. *Cancer Res.* **2009**, *69*, 6232−6240.
(21) Chresta, C. M.; Davies, B. R.; Hickson, I.; Harding, T.; Cosulich, S.; Critchlow, S. E.; Vincent, J. P.; Ellson, R.; Jones, D.; Sini, P.; James, D.; Howard, Z.; Dudley, P.; Hughes, G.; Smith, L.; Maguire, S.; Hummersone, M.; Malagu, K.; Menear, K.; Jenkins, R.; Jacobsen, M.; Smith, G. C. M.; Guichard, S.; Pass, M. AZD8055 Is a Potent, Selective, and Orally Bioavailable ATP-Competitive Mammalian Target of Rapamycin Kinase Inhibitor with in Vitro and in Vivo Antitumor Activity. *Cancer Res.* **2010**, *70*, 288−298.
(22) Menear, K. A.; Gomez, S.; Malagu, K.; Bailey, C.; Blackburn, K.; Cockcroft, X.; Ewen, S.; Fundo, A.; Gall, A. L.; Hermann, G.; Sebastian, L.; Sunose, M.; Presnot, T.; Torode, E.; Hickson, I.; Martin, N. M.; Smith, G. C. M.; Pike, K. G. Identification and Optimization of Novel and Selective Small Molecular Weight Kinase Inhibitors of mTOR. *Bioorg. Med. Chem. Lett.* **2009**, *19*, 5898−5901.
(23) Verheijen, J. C.; Richard, D. J.; Curran, K.; Kaplan, J.; Lefever, M.; Nowak, P.; Malwitz, D. J.; Brooijmans, N.; Toral-Barza, L.; Zhang, W. G.; Lucas, J.; Hollander, I.; Ayral-Kaloustian, A.; Mansour, T. S.; Yu, K.; Zask, A. Discovery of 4-Morpholino-6-aryl-1*H*-pyrazolo[3,4-*d*]pyrimidines as Highly Potent and Selective ATP-Competitive Inhibitors of the Mammalian Target of Rapamycin (mTOR): Optimization of the 6-Aryl Substituent. *J. Med. Chem.* **2009**, *52*, 8010−8024.
(24) Liu, Q.; Wang, J.; Kang, S. A.; Thoreen, C. C.; Hur, W.; Ahmed, T.; Sabatini, D. M.; Gray, N. S. Discovery of 9-(6-Aminopyridin-3-yl)-1-(3-(trifluoromethyl)phenyl)benzo[*h*][1,6]naphthyridin-2(1*H*)-one (Torin2) as a Potent, Selective, and Orally Available Mammalian Target of Rapamycin (mTOR) Inhibitor for Treatment of Cancer. *J. Med. Chem.* **2011**, *54*, 1473−1480.
(25) Mortensen, D. S.; Perrin-Ninkovic, S. M.; Harris, R.; Lee, B. G. S.; Shevlin, G.; Hickman, M.; Khmbatta, G.; Bisonette, R. R.; Fultz, K. E.; Sankar, S. Discovery and SAR Exploration of a Novel Series of Imidazo[4,5-*b*]pyrazin-2-ones as Potent and Selective mTOR Kinase Inhibitors. *Bioorg. Med. Chem. Lett.* **2011**, *21*, 6793−6799.
(26) Cohen, F.; Bergeron, P.; Blackwood, E.; Bowman, K. K.; Chen, H.; DiPasquale, A. G.; Epler, J. A.; Koehler, M. F. T.; Lau, K.; Lewis, C.; Liu, L.; Ly, C. Q.; Malek, S.; Nonomiya, J.; Ortwine, D. F.; Pei, Z.; Robarge, K. D.; Sideris, S.; Trinh, L.; Truong, T.; Wu, J.; Zhao, X.; Lyssikatos, J. P. Potent, Selective, and Orally Bioavailable Inhibitors of Mammalian Target of Rapamycin (mTOR) Kinase Based on a

Quaternary Substituted Dihydrofuropyrimidine. *J. Med. Chem.* **2011**, *54*, 3426−3435.
(27) Maira, S.-M.; Stauffer, F.; Brueggen, J.; Furet, P.; Schnell, C.; Fritsch, C.; Brachmann, S.; Chène, P.; De Pover, A.; Schoemaker, K.; Fabbro, D.; Gabriel, D.; Simonen, M.; Murphy, L.; Finan, P.; Sellers, W.; García-Echeverría, C. *Mol. Cancer Ther.* **2008**, *7*, 1851−1863.
(28) For an example of the use of PC3 cells to evaluate mTOR activity, see: Dan, H. C.; Adli, M.; Baldwin, A. S. Regulation of Mammalian Target of Rapamycin Activity in PTEN-Inactive Prostate Cancer Cells by I κB Kinase α. *Cancer Res.* **2007**, *67*, 6263−6269.
(29) Anand, N. K.; Arcalas, A.; Blazey, C. M.; Buhr, C. A.; Cannoy, J.; Ephsteyn, S.; Johnson, H. W.B.; Joshi, A.; Kim, B. G.; Leahy, J. W.; Lee, M. S.; Ma, S.; Mac, M. B.; Nuss, J. M.; Takeuchi, C. S.; Wang, L.; Wang, Y. Benzoxazepin-4-(5*H*)-yl Derivatives and Their Use To Treat Cancer. PCT Int Appl. WO2010118208A1, 2010.
(30) For an example of the use of this straightforward method for the analysis of the kinetics of enzyme reactions, see: Krohn, K. A.; Link, J. M. Interpreting Enzyme and Receptor Kinetics: Keeping It Simple, but Not Too Simple. *Nucl. Med. Biol.* **2003**, *30*, 819−826.
(31) For an example of the use of MCF7 cells to evaluate mTOR activity, see: Yu, K.; Toral-Barza, L.; Discafani, C.; Zhang, W.-G.; Skotnicki, J.; Frost, P.; Gibbons, J. J. mTOR, a Novel Target in Breast Cancer: The Effect of CCI-779, an mTOR Inhibitor, in Preclinical Models of Breast Cancer. *Endocr.-Relat. Cancer* **2001**, *8*, 249−258.
(32) Huckle, D.; Lockhart, I. M.; Wright, M. The Preparation of Some 2,3-Dihydro-1,4-benzoxazepin-5(4*H*)-ones and Related Compounds. *J. Chem. Soc.* **1965**, 1137−1141.
(33) Vernier, J. M.; Ripka, W.; May, J.; Bounaud, P.; O'Connor, P.; Hopkins, S.; Burkel, H. Antitumor Hedgehog Signaling Inhibitors. PCT Int Appl. WO2011014888A1, 2011.
(34) Zou, G.; Reddy, Y. K.; Falck, J. R. Ag(I)-Promoted Suzuki−Miyaura Cross-Couplings of *n*-Alkylboronic Acids. *Tetrahedron Lett.* **2001**, *42*, 7213−7215.
(35) Yin, J.; Zhao, M. M.; Huffman, M. A.; McNamara, J. M. Pd-Catalyzed *N*-Arylation of Heteroarylamines. *Org. Lett.* **2002**, *4*, 3481−3484.
(36) Ibrahim, M. A.; Johnson, H. W. B.; Jeong, J. W.; Lewis, G. L.; Shi, X.; Noguchi, R. T.; Williams, M.; Leahy, J. W.; Nuss, J. M.; Woolfrey, J.; Banica, M.; Bentzien, F.; Chou, Y.-C.; Gibson, A.; Heald, N.; Lamb, P.; Mattheakis, L.; Matthews, D.; Shipway, A.; Wu, X.; Zhang, W.; Zhou, S.; Shankar, G. Discovery of a Novel Class of Potent and Orally Bioavailable Sphingosine 1-Phosphate Receptor 1 Antagonists. *J. Med. Chem.* **2012**, *55*, 1368−1381.
(37) Leahy, J. W.; Buhr, C. A.; Johnson, H. W. B.; Kim, B. G.; Baik, T.; Cannoy, J.; Forsyth, T. P.; Jeong, J. W.; Lee, M. S.; Ma, S.; Noson, K.; Wang, L.; Williams, M.; Nuss, J. M.; Brooks, E.; Foster, P.; Goon, L.; Heald, N.; Holst, C.; Jaeger, C.; Lam, S.; Lougheed, J.; Nguyen, L.; Plonowski, A.; Song, J.; Stout, T.; Wu, X.; Yakes, M. F.; Yu, P.; Zhang, W.; Lamb, P.; Raeber, O. Discovery of a Novel Series of Potent and Orally Bioavailable Phosphoinositide 3-Kinase γ Inhibitors. *J. Med. Chem.* **2012**, *55*, 5467−5482.